



Macrocyclic oligomers as compatibilizing agent for hemp fibres/biodegradable polyester eco-composites

DOI:

[10.1016/j.polymer.2018.05.053](https://doi.org/10.1016/j.polymer.2018.05.053)

Document Version

Accepted author manuscript

[Link to publication record in Manchester Research Explorer](#)

Citation for published version (APA):

Conzatti, L., Brunengo, E., Utzeri, R., Castellano, M., Hodge, P., & Stagnaro, P. (2018). Macrocyclic oligomers as compatibilizing agent for hemp fibres/biodegradable polyester eco-composites. *Polymer*, 146, 396-406. <https://doi.org/10.1016/j.polymer.2018.05.053>

Published in:

Polymer

Citing this paper

Please note that where the full-text provided on Manchester Research Explorer is the Author Accepted Manuscript or Proof version this may differ from the final Published version. If citing, it is advised that you check and use the publisher's definitive version.

General rights

Copyright and moral rights for the publications made accessible in the Research Explorer are retained by the authors and/or other copyright owners and it is a condition of accessing publications that users recognise and abide by the legal requirements associated with these rights.

Takedown policy

If you believe that this document breaches copyright please refer to the University of Manchester's Takedown Procedures [<http://man.ac.uk/04Y6Bo>] or contact uml.scholarlycommunications@manchester.ac.uk providing relevant details, so we can investigate your claim.



Manuscript Number: POLYMER-18-340R1

Title: Macrocyclic oligomers as compatibilizing agent for hemp
fibres/biodegradable polyester eco-composites

Article Type: Research Paper

Section/Category: Polymer Synthesis

Keywords: entropically-driven ring-opening polymerization (ED-ROP);
macrocyclic oligomers (MCOs); hemp fibres eco-composites

Corresponding Author: Dr. Lucia Conzatti, Ph. D.

Corresponding Author's Institution: Consiglio Nazionale delle Ricerche

First Author: Lucia Conzatti, Ph. D.

Order of Authors: Lucia Conzatti, Ph. D.; Elisabetta Brunengo; Roberto
Utzeri; Maila Castellano; Philip Hodge; Paola Stagnaro

Abstract: Ring:chain equilibria (RCE), existing under appropriate reaction conditions, between a linear polyester and the corresponding family of macrocyclic oligomers (MCOs), were exploited to develop an original compatibilizing pathway for preparing eco-composites based on hemp fibres and a biodegradable random co-polyester, namely poly(1,4-butylene adipate-co-terephthalate) (PBAT) with 50:50 adipate:terephthalate proportion. Cyclo-depolymerization (CDP) of PBAT was successfully carried out at high dilution using various solvents, catalysts, and reaction times. The reconversion of MCOs into linear chains by entropically-driven ring-opening polymerization (ED-ROP) occurs by simple heating in the bulk. This reaction, after optimization of catalyst amount, temperature, and reaction time, was used for the surface modification of hemp fibres. PBAT-based eco-composites containing hemp fibres as such or pre-modified by treatment with the MCOs were then prepared and characterized by morphological and mechanical analysis.



Consiglio Nazionale delle Ricerche

ISMAC - ISTITUTO PER LO STUDIO DELLE MACROMOLECOLE

GENOVA

Via De Marini, 6 - 16149 GENOVA Italy - Tel. (39) 0106475879 - Fax (39) 0106475880

Codice fiscale 80054330586 - Partita Iva 02118311006

Dear Editor,

I am sending the revised version of the manuscript POLYMER-18-340 "*Macrocyclic oligomers as compatibilizing agent for hemp fibres/biodegradable polyester eco-composites*" by L. Conzatti, E. Brunengo, R. Utzeri, M. Castellano, P. Hodge, and P. Stagnaro.

It has been revised according to the referees' comments: the whole text was improved whenever needed and the results obtained by thermogravimetric and dynamic-mechanical analysis of the eco-composites were added. All the revisions done are evidenced in red color.

We have answered all the remarks, as you can see in the attached "Response to Reviewers" file.

We warmly thank the referees for the suggestions aimed at improving the paper.

On behalf of all the authors, I warmly hope the paper can now deserve consideration for publication in **Polymer** journal.

Thank you in advance for your kind attention. Looking forward to hearing from you.

Sincerely yours,

Lucia Conzatti

Genova, May 11th, 2018

Ms. No. POLYMER-18-340

“Macrocyclic oligomers as compatibilizing agent for hemp fibres/biodegradable polyester eco-composites”

Response to Reviewers

Point-by-point the response to Reviewers is given in red in the following.

Reviewer #1 (Major Revision):

This work is very interesting in line with the current trends in biodegradable plastics and natural reinforcing fillers. The modification part is novel and the results are thoroughly presented.

We warmly appreciate the positive comments of the Reviewer on the work in the whole.

However, there some modification which will make this article much more useful to the readers.

1. *Thermal properties of the composites may be added.*

Experimental setup used thermogravimetric analysis (TGA) of the composites, results obtained from and related comments were added in the Manuscript at Pag. 7 – Lines 200-204, at Pag. 16 – Lines 372-379, and at Pag. 20-21 – Lines 464-476.

For homogeneity purposes, also TGA data under N₂ atmosphere of the fibres were reported in Table 3 of the revised Manuscript (Table 3, Pag. 17 – Lines 381-383).

2. *The tensile strain decreased in the sample containing the MCO-modified fibres, how the explain effectiveness of the system to be at best at this composition as normally tensile strain is used to indicate the compatibility between matrix-filler.*

To answer to this point, the following sentence was added at Pag. 21-22 – Lines 490-495:

“The slight decrease of the stress at break could be ascribed to a mechanical weakening of the hemp fibres due to the thermal treatment carried out during the ED-ROP reaction (190°C, 30 min). Even though a TGA isothermal analysis carried out at 200°C in O₂ atmosphere for 30 min revealed a good thermo-oxidative resistance of HF_{Na}s fibres (the weight loss is about 0.5%), the maintenance at high temperature in oxidative atmosphere could be slightly detrimental to the mechanical properties of the fibres, as reported by Prasad *et al.* [34].”

Moreover, in order to further support the enhanced fibre-PBAT adhesion/interaction due to the presence of MCOs, DMA tests were also carried out. Related data and comments were added in the revised Manuscript at Pag. 7 – Lines 208-210 and 217-223, and at Pag. 22 – Lines 496-515.

3. *The composite at various compositions may be prepared and characterized for their mechanical properties.*

The study of composites at various fibre composition is out of the scope of the present Manuscript, which is that of demonstrate the upcycling of HF residues on evaluating the efficiency of MCO as compatibilizing agent in PBAT-based eco-composites. For this purpose, such a high amount (about 40 wt.-%) of HF was added to the PBAT matrix.

The study of eco-composites with different amounts of fibres will be the object of a future work.

Reviewer #2 (Reject):

1. *The reaction formula of MCO should be added.*

The scheme of the ring:chain equilibrium of MCOs vs. PBAT was added (Scheme 2) in the text at Pag. 3 – Lines 85-86.

2. *Why did the authors choose such a polyester with so wide PDI, about 8?*

This polyester grade was suggested from BASF technical personnel as the most suitable for the preparation of eco-composites by melt blending technique.

3. *In page 11, "the low melting range confirms the considerations on the relative volatility of the MCOs previously done". What's the relationship between the melting point and the volatility of MCOs? The DSC and TGA curves of MCOs are recommended to be added in the supporting information.*

We agree with the referee: the relationship between the melting point and the volatility of MCOs is not directly proportional. However, DSC heating curve of MCOs shows a broad endothermic peak ranging from 30 to 60°C indicating a very low melting point. The relative volatility of MCOs could be enhanced in the conditions used for the removal of the *o*-DCB solvent, during which they were maintained at relatively high temperature (70°C) under vacuum. Moreover, it is to be outlined that the most volatile one is expected to be the monomeric cyclic *n*-butyl adipate.

A sentence was added at Pag. 9 – Lines 258-259 and that at Pag. 11 – Lines 288-289 was properly modified as "(this low melting range supports the considerations on the relative volatility of the MCOs previously done)".

Actually, DSC analyses were carried out, even though the related curves are not shown because they lack of significance in the Manuscript context. In facts, ED-ROP of MCOs takes place during the DSC (or TGA) heating run resulting in a dynamic system which leads to the PBAT formation.

4. *In page 19, "HFNa_s, that only exhibits a feeble signal ascribable to carbonyl groups centred at 1735 cm⁻¹". However, as shown in Figure 9, there is no peak at 1725 for the curve of HFNa_s, but there is a peak at around 1690.*

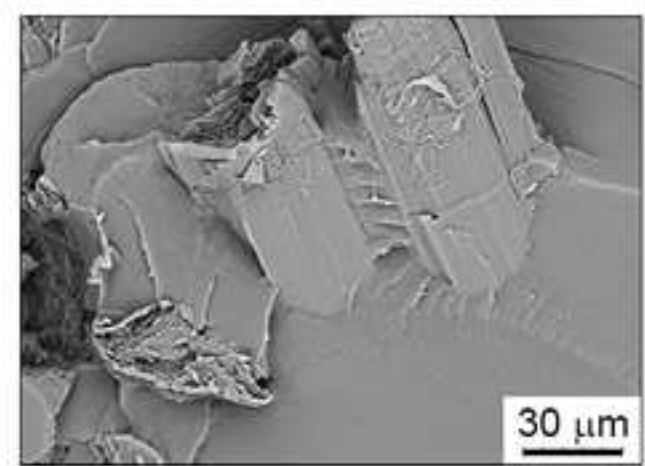
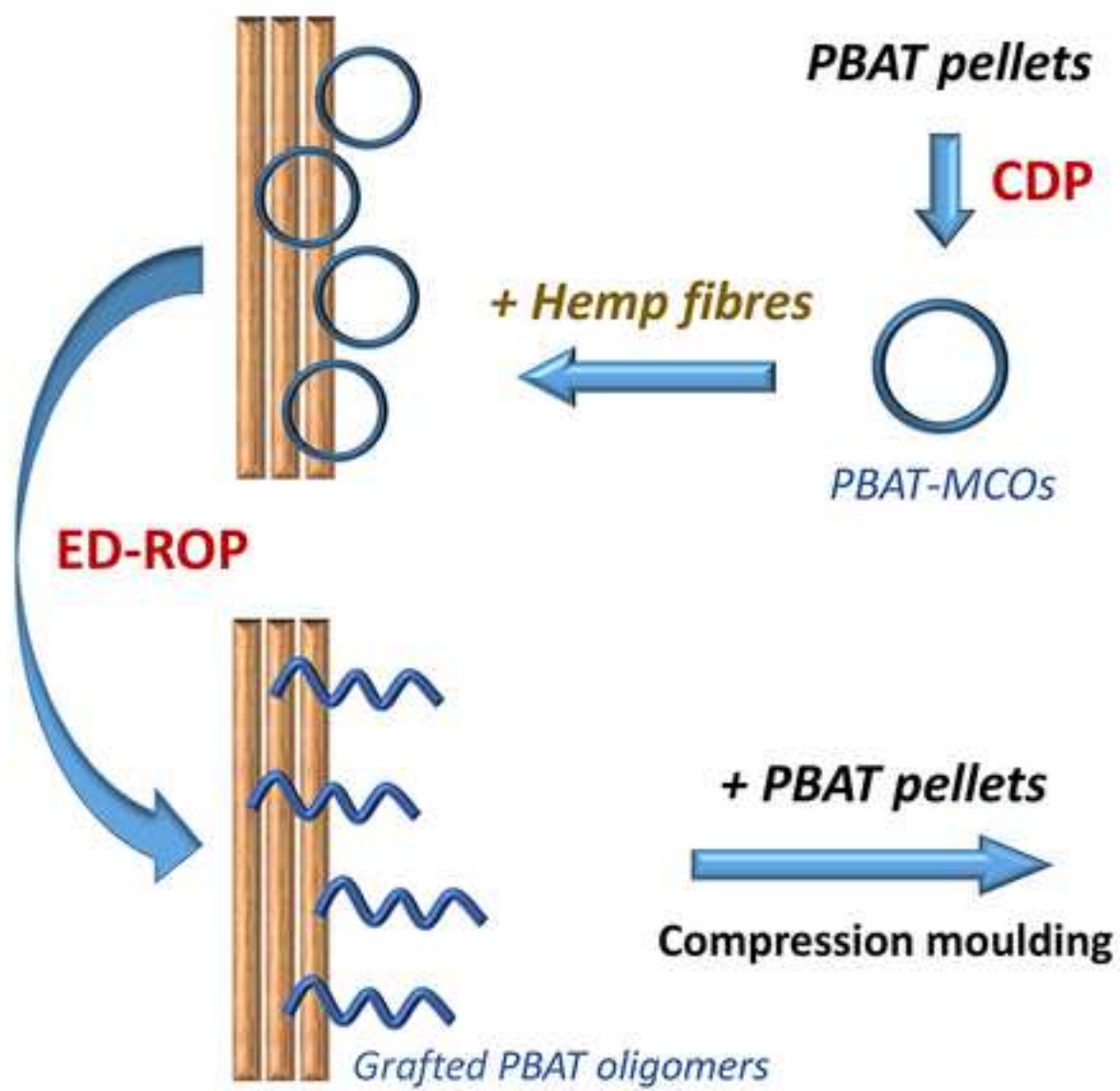
The authors thank the referee for the suggestion, Figure 9 and relative caption (Pag. 18 – Lines 414-418) were improved inserting an inset to help the readers.

5. *In page 22, although the storage modulus (*E*) of PBAT + HFNa-*np*MCOs is larger than that of PBAT + HF_s, the stress at break ($\langle \sigma \rangle_b$) and the elongation at break ($\langle \xi \rangle$) are lower obviously. Why?*

To answer to this point, the following sentence was added at Pag. 21-22 – Lines 490-495:

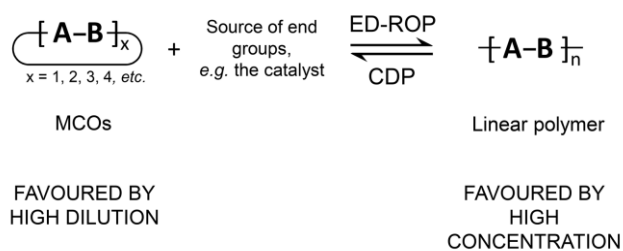
"The slight decrease of the stress at break could be ascribed to a mechanical weakening of the hemp fibres due to the thermal treatment carried out during the ED-ROP reaction (190°C, 30 min). Even though a TGA isothermal analysis carried out at 200°C in O₂ atmosphere for 30 min revealed a good thermo-oxidative resistance of HF_{Na}_s fibres (the weight loss is about 0.5%), the maintenance at high temperature in oxidative atmosphere could be slightly detrimental to the mechanical properties of the fibres, as reported by Prasad *et al.* [34]."

Moreover, in order to further support the enhanced fibre-PBAT adhesion/interaction due to the presence of MCOs, DMA tests were also carried out. Related data and comments were added in the revised Manuscript at Pag. 7 – Lines 208-210 and 217-223, and at Pag. 22 – Lines 496-515.



35 1. Introduction

36 In the last decade, macrocyclic oligomers (MCOs) and their entropically-driven ring-opening
37 polymerization (ED-ROP) have become of interest for the synthesis of polycondensation polymers
38 such as polyesters, polycarbonates, certain polyamides, and various high-performance aromatic
39 polymers [1-3]. ED-ROPs are based on ring:chain equilibria (RCE), *i.e.* the well-known equilibria
40 existing, under appropriate reaction conditions, between a condensation polymer and the
41 corresponding family of MCOs (Scheme 1) [1,2,4].



43
44 **Scheme 1.** A generalized ring:chain equilibrium. (1-column fitting image)

45
46 ED-ROP can be considered as a green process because to push the equilibrium towards the linear
47 polymer generally no solvent is required, and, since the starting MCOs have no end groups and are
48 strainless, no small molecules are released and little or no heat is evolved. Furthermore, high-
49 molecular-weight polymers can be prepared in relatively short reaction times under atmospheric
50 pressure, and the lower melt viscosity of the MCOs with respect to the polymer being formed
51 allows easier processing by various techniques, such as pultrusion, resin-transfer moulding, reaction
52 injection moulding, either concurrent with or just prior to polymerization [5-7]. ED-ROP has
53 potential application in the preparation of composite materials [3], as voids due to the release of
54 small volatile compounds are not created in the final products and the control of temperature
55 throughout the reaction course is relatively facile.

56 In a wider context, growing global environmental and social concerns, high rate of depletion of
57 petroleum resources, and new environmental regulations have encouraged the search for green
58 processes, and in this respect, ED-ROP of strainless MCOs appears perfectly suited [1,2].

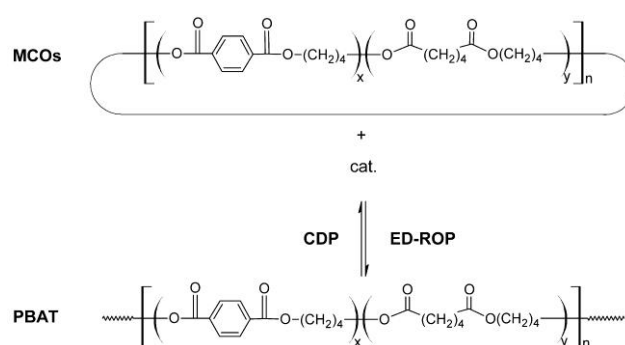
59 Furthermore, the interest for new materials derived from renewable sources as well as for recycle
60 and valorization of low cost, waste or difficult-to-dispose natural products, such as wool or ligno-
61 cellulosic fibres obtained from the stem of hemp, flax, jute, bamboo, etc. [8-12] is continuously
62 increasing. In this field, many scientific research projects, as well as many commercial programs,
63 are nowadays focused on eco-composites, *i.e.* composite materials, based on natural fibres
64 embedded in natural or biodegradable polymer matrices [9,11], that can be easily degraded or bio-

65 assimilated, thus possessing environmental and ecological advantages over conventional
66 composites. In particular, eco-composite materials containing ligno-cellulosic natural fibres (hemp,
67 flax, jute, etc.) are characterized by low density, low environmental impact, recyclability and
68 favourable cost/performance ratio [8,10,12].

69 Ligno-cellulosic fibres, which mainly consist of cellulose filaments embedded in a matrix of
70 hemicellulose and lignin, have pronounced hydrophilic characteristics. This generally leads to a
71 poor fibre-polymer interaction since the polymer matrix is typically apolar or only weakly polar. As
72 a consequence, the attainment of eco-composites with good mechanical properties requires
73 improvement in the compatibility between the two components [8,10,12,13].

74 Within this framework, in recent years we have started a study aimed at improving the adhesion
75 between natural fibres (in particular wool) and various polymer matrices [14-17], exploring
76 different compatibilization strategies.

77 In the present work the ED-ROP of the MCOs, obtained by cyclo-depolymerization (CDP) of a
78 commercial biodegradable random co-polyester, namely poly(1,4-butylene
79 adipate-*co*-terephthalate) (PBAT) (50:50 adipate:terephthalate), was exploited to develop a novel
80 compatibilization pathway for achieving eco-composites based on PBAT and hemp fibres (HFs). As
81 a matter of fact, the MCOs, previously adsorbed onto the hemp fibres and converted into oligomeric
82 chains by ED-ROP (Scheme 2), can act as a compatibilizing agent capable, at least in principle, of
83 interacting with both the fibre surface and the polyester matrix directly during melt mixing and/or
84 by proper thermal treatments.



85
86 **Scheme 2. Ring:chain equilibrium of PBAT. (1-column fitting image)**

87
88 To this purpose, CDP of PBAT polyester was investigated at high dilution by varying the solvent,
89 the catalyst and/or the reaction time. Selected MCOs were then used to optimize the conditions of
90 the ED-ROP and then pre-adsorbed onto HFs previously mildly treated with aqueous NaOH. Once
91 the ED-ROP of the MCOs adsorbed onto HFs has taken place, the uncut fibres were combed and
92 incorporated into the PBAT matrix by compression moulding. The ensuing eco-composites were

93 then morphologically characterized to evaluate the fibre-matrix interaction and subjected to
94 preliminary uniaxial tensile tests to investigate their mechanical properties.

95

96 **2. Materials and methods**

97 *2.1. Materials*

98 A commercial biodegradable, statistical poly(1,4-butylene adipate-*co*-terephthalate) (PBAT) grade
99 (Ecoflex® F Blend A1200), kindly supplied by BASF (Germany), was used as the polyester matrix.

100 $\overline{M}_n = 11.7 \cdot 10^3$ g/mol and $\overline{M}_w = 84.4 \cdot 10^3$ g/mol were evaluated by size exclusion
101 chromatography (SEC). Values of $T_g = -33^\circ\text{C}$, $T_m = 118^\circ\text{C}$, $\Delta H_m = 26$ J/g, $T_c = 30^\circ\text{C}$ and $\Delta H_c = 24$
102 J/g were determined by differential scanning calorimetry (DSC). See the paragraph 2.6 for details
103 on experimental conditions. The proportion of adipate versus terephthalate units was about 1:1, as
104 determined by ^1H NMR analysis.

105 Raw hemp fibres of *Carmagnola* type, from which shives had been previously removed, were
106 kindly supplied by Assocanapa (Italy) and used as received (HFs) or mildly treated (HF_{NaS}) in an
107 aqueous solution of NaOH (0.2% wt./v) at 20°C for 48 h, following a procedure analogous to that
108 reported in the literature [18].

109 Except where indicated otherwise, chemicals were purchased from Sigma-Aldrich and used as
110 received.

111

112 *2.2. Preparation of the MCOs*

113 MCOs were obtained from PBAT by CDP at high dilution (1% wt./v), at solvent reflux temperature
114 and in the presence of 3 mol% of a transesterification catalyst (namely *n*-dibutyltin(IV) oxide, *n*-
115 Bu₂SnO, or titanium(IV) 2-ethylhexyloxyde, Ti(OR)₄), by adapting a procedure already described
116 for other polyesters [3,7]. *o*-Dichlorobenzene (DCB) or CHCl₃ were used as the solvent. The work
117 up adopted for CDPs in DCB involved the solvent removal by rotoevaporation at 70°C and 2-3
118 mmHg followed by drying in a vacuum oven to constant weight. In the case of CHCl₃, the CDP
119 products were recovered by solvent evaporation at room temperature in a fume hood, followed by
120 careful drying under mild conditions. The CDP yield was determined as weight percentage with
121 respect to the initial amount of PBAT. Reaction times were varied from 3 to 5 days.

122 The MCOs obtained from the CDP carried out under optimized conditions were used as such (that
123 is non-purified: these are labelled npMCOs in the following where appropriate) or were purified by
124 dissolution in the minimum amount of CHCl₃ and elution with CH₂Cl₂/acetone 94/6 v/v through a
125 column of activated basic Al₂O₃ (150 mesh). Effective purification was checked by thin layer

126 chromatography (TLC), elemental analysis and SEC. Purified MCOs were labelled pMCOs in the
127 following where appropriate.

128 Before use MCOs were stored under vacuum in anhydrous conditions.

129

130 2.3. ED-ROP of MCOs

131 ED-ROPs were carried out on the MCOs in isothermal conditions in a DSC pan. Samples (about 10
132 mg) were rapidly heated up to the selected temperature. The amount of *n*-Bu₂SnO catalyst (0-3
133 mol% with respect to the MCOs), reaction time (8-120 min) and temperature (180-200°C) were
134 varied. The products obtained from the ED-ROPs were then characterized by SEC and DSC and
135 compared with the commercial PBAT.

136

137 2.4. Modification of hemp fibres with the MCOs

138 On alkali treated HF_{Na}S two modification procedures were performed as follows: (i) npMCOs were
139 pre-adsorbed onto HF_{Na}S (HF_{Na}-npMCOs) by immersing the fibres in a CHCl₃ solution (5% wt./v)
140 of npMCOs; or (ii) *n*-Bu₂SnO was previously adsorbed onto HF_{Na}S through immersion of the fibres
141 in a CHCl₃ solution (0.18% wt./v) of the catalyst and, after CHCl₃ evaporation, pMCOs were added
142 as described for (i), obtaining fibres labelled HF_{Na}-C-pMCOs.

143 After CHCl₃ evaporation, the MCOs pre-adsorbed on the fibres underwent ED-ROP by simple
144 heating in a P200E semi-automatic hot-plate press (Collin GmbH). For HF_{Na}-npMCOs ED-ROPs
145 were carried out at 190 or 200°C for 30 or 120 min, while 190°C and 30 min were the conditions
146 adopted for HF_{Na}-C-pMCOs. The so obtained fibres were then washed several times with CHCl₃ to
147 remove ungrafted oligoester chains until TLC of the extracts did not reveal any trace of unreacted or
148 ungrafted products. Extracts were analyzed by Fourier transform infrared spectroscopy (FTIR) and
149 SEC.

150 A higher amount of HF_{Na}-npMCO fibres was obtained by fixing uncut, combed and slightly
151 stretched HF_{Na} fibres to a frame and immersing them in a CHCl₃ solution (2.5% wt./v) of npMCOs
152 (30 wt.% MCOs *vs.* fibres). After solvent evaporation at room temperature and pressure, ED-ROP
153 of the pre-adsorbed npMCOs was performed at 190°C for 30 min. The ensuing HF_{Na}-npMCO fibres
154 were carefully washed with CHCl₃ and dried at 60°C in a ventilated oven.

155

156 2.5. Preparation of hemp fibre/PBAT composites

157 Preliminary PBAT-based composites containing low amounts (less than 5 wt.%) of HF, HF_{Na},
158 HF_{Na}-C-pMCO, or HF_{Na}-npMCO fibres were prepared by placing slightly stretched fibres between

159 two 0.3 mm thick sheets of PBAT and by moulding the resulting “sandwich” in the semi-automatic
160 press at 180 °C, *i.e.* above T_m , for 1 min at 5 bar and then 4 min at 160 bar.

161 PBAT-based composites (10x10x0.1 cm sheets) containing higher amounts (about 40 wt.%) of
162 uncut oriented HF, HF_{Na}, and HF_{Na}-npMCO fibres were then prepared by compression moulding
163 through a two-step method: (i) impregnation of combed and slightly stretched fibres into melted
164 PBAT (180°C, 8 min) and achievement of sheets by moulding at 180°C, 1 MPa, 7 min; (ii)
165 moulding (150°C, 1 MPa, 3 min) two so-obtained sheets with fibres oriented in the same direction.

166

167 2.6. Characterizations

168 SEC analyses were carried out using a Perkin Elmer chromatography system with a Diode Array
169 Detector 235C and operating at a flow rate of 1 mL/min. CHCl₃ was used both as solvent and
170 eluent. Column set: 10³ (PL GEL, 30 cm, 5 µm), 500 Å (PL GEL, 30 cm, 5 µm), 500 Å (PL GEL,
171 30 cm, 10 µm), 100 Å (Styragel HR1, 30 cm, 5 µm). PBAT pellets were analysed with the
172 following column set: 10⁵ (Styragel HR5, 30 cm, 5 µm), 10⁴, 10³, 500 Å (PL GEL, 30 cm, 5 µm).

173 TLC analysis was carried out by using CH₂Cl₂/acetone 94/6 v/v as eluent.

174 Elemental analysis was carried out by inductively coupled plasma-optical emission spectroscopy
175 (ICP-OES) using a Fisons Instruments Horizon instrument to evaluate Sn content in selected MCOs
176 samples.

177 Room temperature ¹H NMR spectrum of PBAT dissolved in deuteriochloroform (CDCl₃) was
178 obtained with a Bruker Avance-500 spectrometer (no internal chemical shift reference).

179 FTIR spectroscopic characterization of PBAT, MCOs, fibres, and extracts from the fibre washing
180 was performed with a Perkin Elmer Spectrum Two™ FTIR spectrometer operating in the attenuated
181 total reflectance (ATR) mode and recording absorbance spectra in the wave number range 4000-400
182 cm⁻¹.

183 Room temperature wide angle X-ray diffraction (WAXD) spectra of hemp fibres were obtained
184 using a Siemens diffractometer model D-500 equipped with a Siemens FK 60-10 2000W tube (Cu
185 K_α radiation, λ = 0.154 nm). The operating voltage and current were 40 kV and 40 mA,
186 respectively. Data were collected from 5 to 40° 2θ at 0.02° 2θ intervals. The percentage crystallinity
187 index (*CI*) of cellulose in hemp fibres was determined by extracting the three crystalline peaks
188 between 10 and 30° 2θ from the diffraction intensity profiles with a non-linear curve-fitting process
189 [19,20]. A peak fitting commercial software (OriginPro 2015, OriginLab Co.) was used, assuming
190 for each peak Lorentzian functions. The *CI* was calculated from the ratio of the area of the
191 crystalline peaks to the total area.

192 A Mettler DSC 821^o calorimeter was used for thermal characterization of the materials and for
193 performing small-scale ED-ROPs in the DSC pan. For characterization of the products obtained
194 from CDPs a single heating run between 0 and 200^oC (scan rate 20^oC/min) was performed.
195 Heating-cooling-heating cycles from 0 up to 200^oC (scan rate 20^oC/min) were applied for PBAT
196 pellets and products obtained from ED-ROPs.

197 Thermogravimetric analysis (TGA) measurements were performed with a PerkinElmer TGA7
198 analyzer operating in dynamic mode. Samples of PBAT and fibres of about 10 mg were heated at
199 20 ^oC/min under O₂ from 50 to 900^oC (gas flow rate 40 mL/min). The water content (mass loss at
200 150^oC), the decomposition temperatures corresponding to 5 wt.% mass loss (T_5) and **the maximum**
201 **rate of decomposition (T_{Vmax}) were determined.** Samples of composites of about 10 mg were heated
202 at 10 ^oC/min under N₂ from 30 to 750^oC (gas flow rate 40 mL/min) for the evaluation of the fibre
203 content. **The onset (T_{onset}) and the T_{Vmax} degradation temperatures were determined. For reference**
204 **purpose, neat PBAT and all HFs were analysed in the same experimental conditions.**

205 Morphological analysis was carried out by scanning electron microscopy (SEM) using a Hitachi
206 TM3000 benchtop SEM microscope operating at 15 kV acceleration voltage. Fibres and fragile
207 surfaces of composites fractured in liquid N₂ were sputtered with gold using a Quorum Q150R ES
208 sputter coater (2M Strumenti) at 20 mA for 5 min prior to the observation. **Moreover, a FE-SEM**
209 **Zeiss Supra 40VP was used for a deeper morphological analysis of the samples after dynamic-**
210 **mechanical analysis (DMA).**

211 Uniaxial tensile tests were performed by using a displacement-controlled dynamometer (Instron
212 5565) according to the ASTM D412 TC standard method (25^oC, load cell 5 kN, constant crosshead
213 speed 20 mm min⁻¹) on rectangular specimens (80x10x1 mm). Tensile modulus (E), stress (σ_b) and
214 strain (ϵ_b) at break were evaluated for neat PBAT matrix and its composites with hemp fibres.
215 Mechanical parameters were measured on more than 6 specimens and the average values were
216 calculated.

217 **Dynamic-mechanical measurements were carried out on rectangular specimens (40x10x1 mm) with**
218 **a strain-controlled rotational rheometer MCR301 (Anton Paar). The range of viscoelastic linearity**
219 **was determined through amplitude sweep tests performed at 1 Hz and 25^oC in the strain range**
220 **0.01÷100%; room temperature frequency sweep tests were then carried out in the torsion mode at**
221 **0.1% amplitude deformation in the frequency range 0.1÷50 Hz, both in longitudinal and transversal**
222 **direction (*i.e.*, with fibres parallel or perpendicular to the clamp axis, respectively). Elastic (G') and**
223 **dissipative (G'') components of the modulus were determined.**

224

225

226 3. Results and Discussion

227

228 3.1. CDP of PBAT

229 CDPs of PBAT were carried out by using different solvents (DCB or CHCl₃), catalysts (Ti(OR)₄,
230 with R = 2-ethylhexyl, or *n*-Bu₂SnO) and/or reaction times (3-5 days), as described in the Materials
231 and methods section and summarized in Table 1.

232

233 **Table 1.** CDPs of PBAT carried out at high dilution (1 % wt./v) and SEC characterization.

Run	Solvent	Catalyst	Reaction time (days)	Product Yield ^a (wt.%)	Fraction with Mp < 4000 ^a (%)
1	DCB	Ti(OR) ₄ ^b	3	88	16
2	DCB	Ti(OR) ₄ ^b	4	71	33
3	DCB	<i>n</i> -Bu ₂ SnO	3	25	85
4	CHCl ₃	<i>n</i> -Bu ₂ SnO	5	100	100
5	CHCl ₃	<i>n</i> -Bu ₂ SnO	4	100	100
6	CHCl ₃	<i>n</i> -Bu ₂ SnO	3	100	100

234 ^a Calculated as weight percentage of recovered reaction products with respect to the initial amount
235 of PBAT.

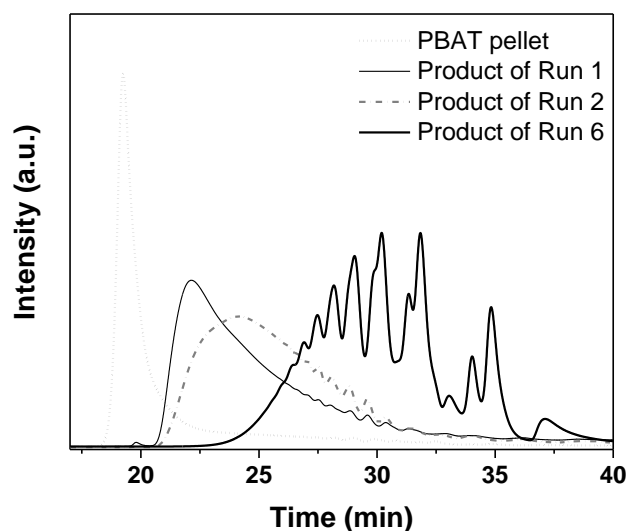
236 ^b Obtained from SEC analysis.

237 ^c R: 2-ethylhexyl.

238

239 The reaction was conveniently monitored by SEC analysis. SEC traces of the starting PBAT pellets
240 and of the equilibrated CDP mixtures obtained under selected experimental conditions are
241 compared in Fig. 1. Depending on reaction conditions, the SEC traces present either a major peak of
242 relatively high molecular weight (Run 1 and 2) or a series of peaks of low molecular weight (Run
243 6). In the former case, CDP of PBAT does not occur to an appreciable extent and PBAT is
244 practically recovered unaltered; in the latter reactions the MCOs are successfully formed, as
245 evidenced by the series of peaks corresponding to MCOs of different ring sizes and, possibly,
246 compositions (since PBAT is a copolyester with aliphatic-aliphatic and aliphatic-aromatic ester
247 linkages having non-identical chemical reactivity). The relative amount of each species present in
248 the reaction product was calculated from the SEC traces as percentage area.

249



250

251 **Fig. 1.** SEC traces of PBAT and some selected products obtained from its CDP. (1-column fitting
252 image)

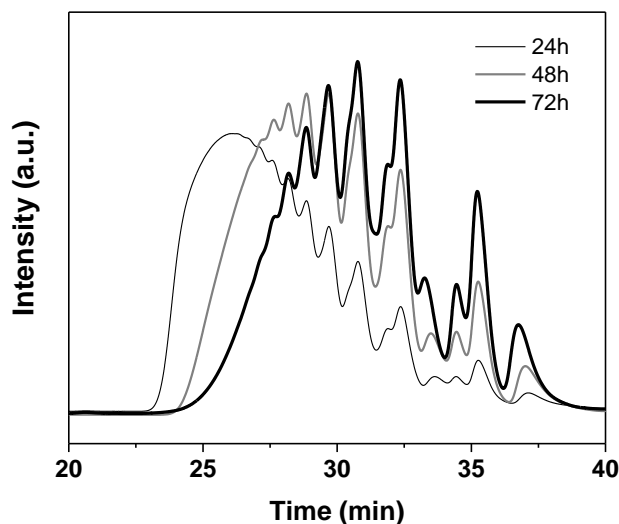
253

254 No significant amounts of low molecular weight species were obtained with the Ti-based catalyst
255 (Run 1 and 2), but MCOs were successfully prepared by CDP in both solvents when *n*-Bu₂SnO was
256 the catalyst. However, when DCB was used as the solvent (Run 3) the work-up following the
257 reaction led to the recovery of a very low amount of MCOs product (25%). This is ascribable to the
258 loss of lower molecular weight fraction of MCOs, **considering that the monomeric cyclic *n*-butyl
259 adipate is expected to be the most volatile one.**

260 By using CHCl₃ as solvent, which has a much lower boiling point than DCB, the work-up was
261 easier, as indicated in the Materials and methods section, and quantitative yields in MCOs were
262 obtained (Run 4-6). The effect of the reaction time was also evaluated carrying out the CDP with
263 the CHCl₃/*n*-Bu₂SnO pair: as evidenced in Table 1 and in Fig. 2, 3 days at reflux temperature are
264 necessary for obtaining the MCOs in high yield (Run 6).

265

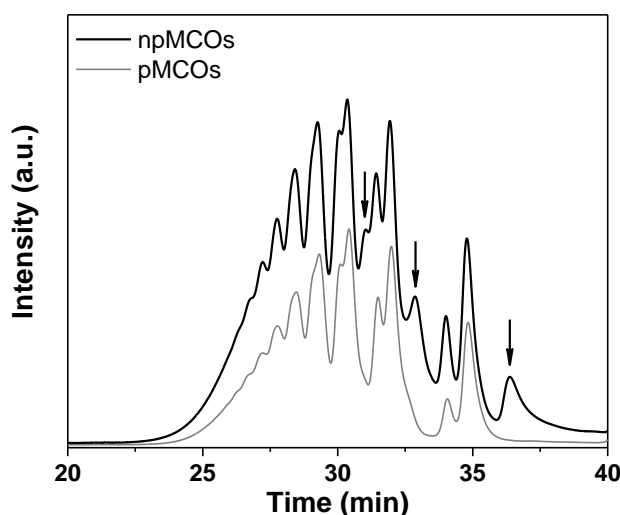
266



267

268 **Fig. 2.** SEC traces of products obtained from CDP of PBAT carried out at different reaction times
 269 (see Table 1, Runs 4-6). (1-column fitting image)

270



271

272 **Fig. 3.** SEC traces of the MCOs obtained as in Run 6 of Table 1, before and after purification. (1-
 273 column fitting image)

274

275 Accordingly, the MCOs obtained from Run 6 were selected to perform successive ED-ROP
 276 experiments and HF modification. The MCOs were used either as directly obtained from the CDP
 277 (npMCOs), or were purified by adsorptive filtration on Al_2O_3 (pMCOs) [7] to remove as much as
 278 possible any residue of transesterification catalyst and possible traces of linear oligomeric species.
 279 A yield of 65 wt.% was found after filtration. TLC carried out on the MCOs before and after
 280 purification indicated the removal of the most polar species. Furthermore, in the SEC traces of
 281 purified MCOs the peaks at 240, 480 and 750 g/mol, probably ascribable to linear oligomeric
 282 species [21], disappeared (Fig. 3 and Table 2). The presence of the tin-based catalyst used for the

283 CDP was checked by elemental analysis for Sn both in npMCOs and pMCOs. A content of 1.44
 284 wt.% of Sn (that corresponds to the 3 mol% catalyst introduced) was found in npMCOs, which
 285 were isolated without any washing after CDP; whereas after the filtration on Al₂O₃ practically all
 286 the catalyst was removed from pMCOs, since only traces (< 0.1%) of tin were detected.
 287 DSC analysis showed a similar thermal behaviour for the MCOs both before and after purification.
 288 Thus, a broad endothermic peak centred at about 50°C is observed upon heating (this low melting
 289 range supports the considerations on the relative volatility of the MCOs previously done).

290
 291 **Table 2.** SEC Characterization of the MCOs before and after purification.

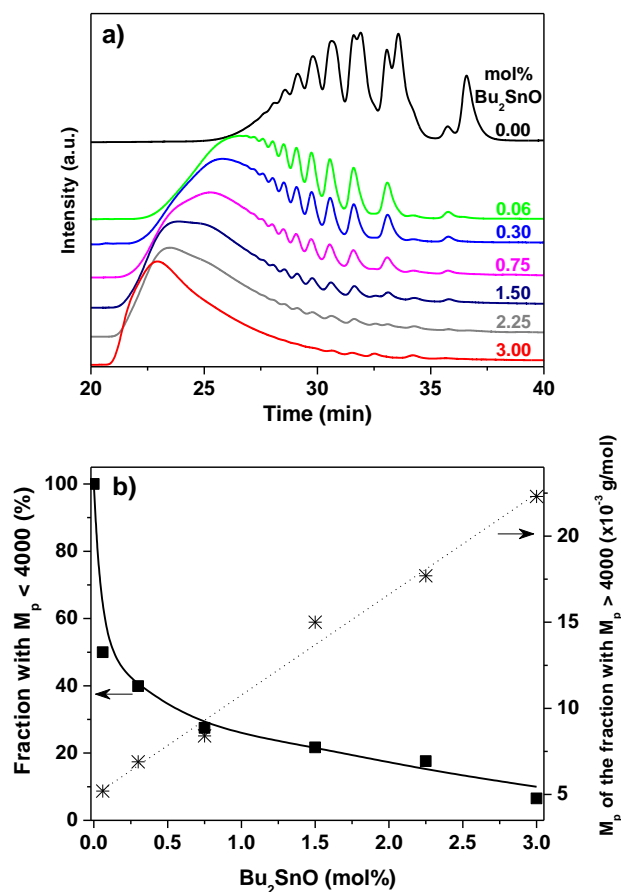
npMCOs		pMCOs	
M_p^a (g/mol)	Area (%)	M_p^a (g/mol)	Area (%)
3930	9.7	3950	9.4
2420	4.8	2410	4.3
2020	6.5	2000	7.8
1630	9.3	1600	11.1
1250	12.4	1230	15.2
990	6.3	980	6.7
910	9.0	900	14.1
750	3.9	-	-
680	6.5	680	6.8
600	10.2	600	14.3
480	6.1	-	-
370	3.5	370	2.3
320	7.0	320	8.1
240	4.8	-	-

292 ^a Molecular weight at peak.

293
 294 **3.2. ED-ROP of the MCOs**

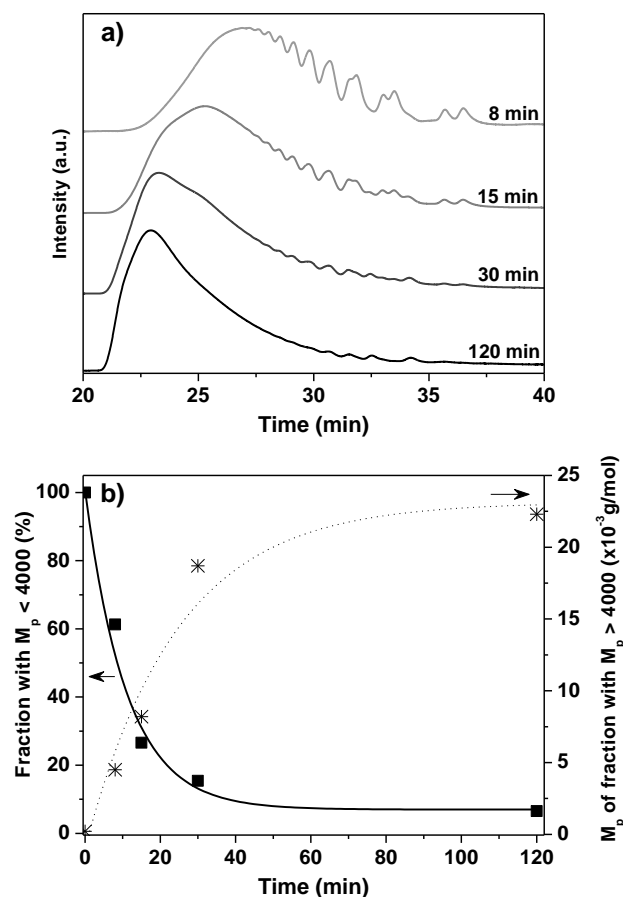
295 Several ED-ROP runs on the MCOs were carried out under N₂ in a pan placed in the DSC furnace
 296 with the aim of investigating the influence of *n*-Bu₂SnO concentration, reaction time and
 297 temperature on molecular and thermal characteristics of the ensuing polyesters. For this purpose,
 298 samples of the MCOs containing different amounts of *n*-Bu₂SnO catalyst were obtained by mixing
 299 solutions (using CHCl₃ as a solvent) of npMCOs, which were assumed to contain unvaried (with
 300 respect to the amount introduced for the CDP) *n*-Bu₂SnO content (3 mol%), and of pMCOs
 301 (assumed to be completely free of catalyst). As shown by SEC traces of Fig. 4, the presence of *n*-

302 Bu_2SnO is necessary for efficient ED-ROPs of MCOs in the selected conditions. Products with
303 higher molecular weights were obtained by increasing the amount of $n\text{-Bu}_2\text{SnO}$.



304
305 **Fig. 4.** SEC traces of products obtained from ED-ROPs of the MCOs (180°C, 120 min) carried out
306 by varying the amount of $n\text{-Bu}_2\text{SnO}$ (a); Plots of M_p and Fraction with $M_p < 4000$ vs. $n\text{-Bu}_2\text{SnO}$
307 amount (b). (1-column fitting image)

308
309 Thus ED-ROP runs were carried out on npMCOs (that is containing 3 mol% $n\text{-Bu}_2\text{SnO}$) varying the
310 reaction time. Data obtained from SEC analysis of ED-ROP products shown in Fig. 5 indicate that
311 ED-ROP of npMCOs takes place to a certain extent already after 8 min and the molecular weight of
312 ED-ROP products being formed increased rapidly in the first 30 min in the DSC pan. Reaction
313 times longer than 30 min did not lead to substantial further increase of the molecular weight of the
314 products.



315
 316 **Fig. 5.** SEC traces of products obtained from ED-ROPs of the MCOs (3 mol% *n*-Bu₂SnO, 180°C)
 317 carried out by varying the reaction time (a); Plots of M_p and Fraction with $M_p < 4000$ vs. reaction
 318 time (b). (1-column fitting image)

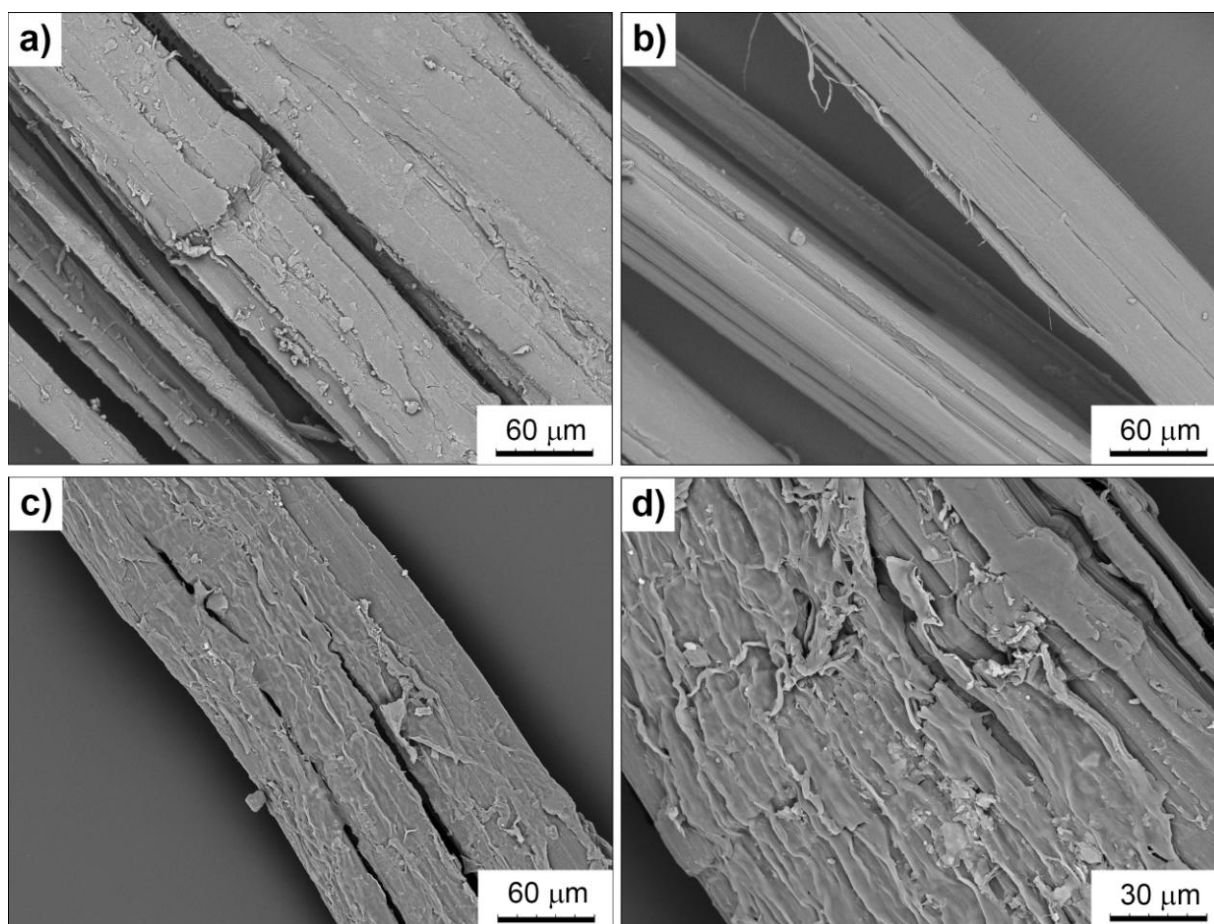
319
 320 ED-ROP runs were finally carried out on npMCOs fixing reaction time at 30 min and varying the
 321 temperature (180, 190, 200°C). Obtained SEC data (not shown here) indicate that for temperatures
 322 higher than 190°C the molecular weight reaches a plateau value of about 21000 g/mol and the
 323 amount of low molecular species is lower than 10%.

324 DSC analysis of the ED-ROP products (data not shown) confirmed the results obtained from SEC
 325 analysis. The product obtained from ED-ROP of npMCOs carried out at 190°C for 30 min presents
 326 a thermal behaviour similar to that of the original PBAT pellets (melting temperature about 120°C).

327 328 3.3. Surface modifications of hemp fibres

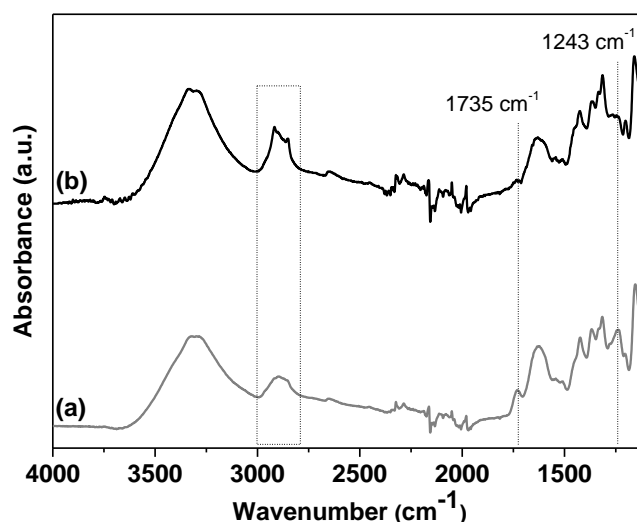
329 Raw hemp fibres, previously freed of shives as indicated in the Materials and methods section, were
 330 considered for the preparation of eco-composites based on Ecoflex®, a commercial grade of the
 331 biodegradable PBAT copolyester. In order to improve their compatibility with the polymer matrix,
 332 the fibres were firstly treated under mild conditions with an aqueous solution of NaOH to make

333 their functional groups more accessible for successive reactions. Natural cellulosic fibres are
334 complex assemblies including cellulose, hemicellulose, lignin, pectin, waxes and water-soluble
335 substances [22]. The removal of the non-cellulosic materials from the fibre surface is beneficial for
336 interaction with polymer matrices and propaedeutic for the successive chemical modification.
337 Among the proposed methods, alkali treatment is widely used for removing non-cellulosic
338 components and part of the amorphous cellulose [23,24]. However, this treatment can significantly
339 modify the crystalline structure of the fibres. The mild conditions adopted in this work for treating
340 HFs [18], resulted in better separated fibres with cleaner surface topography (Fig. 6 a,b) due to a
341 partial removal of non-cellulosic components.



342
343 **Fig. 6.** SEM micrographs of: (a) HFs, (b) HF_{NaS}, and (c,d) HF_{Na}-npMCOs. (2-column fitting image)
344

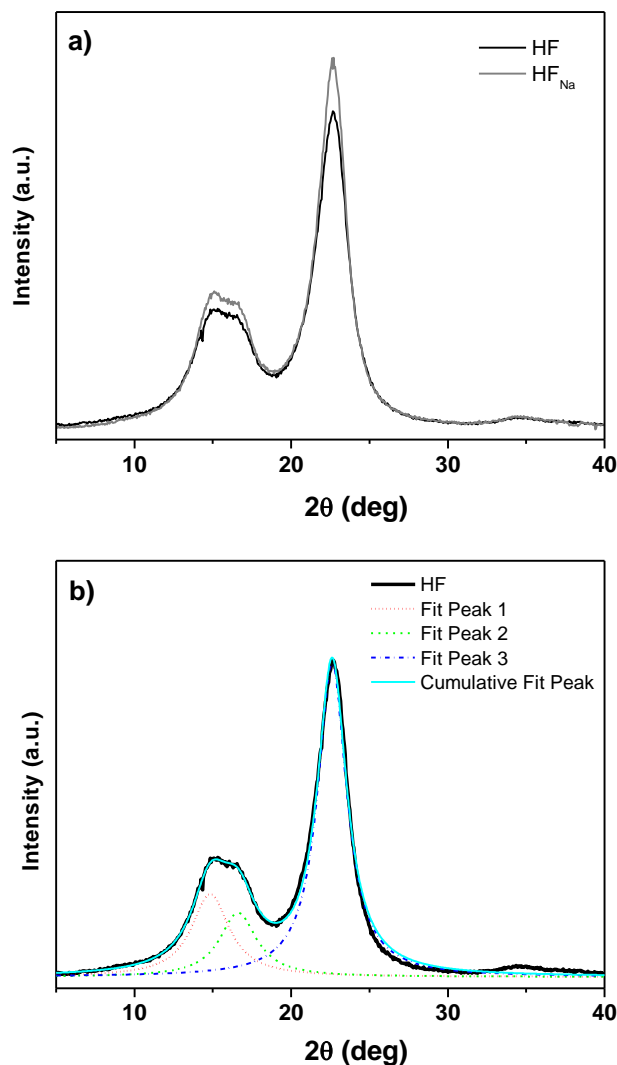
345 ATR-FTIR analysis of HF and HF_{Na} fibres confirmed SEM observations indicating the removal of
346 hemicellulose component as a consequence of the NaOH treatment. In particular, as shown in Fig.
347 7, the intensity of the peak at 1735 cm⁻¹, characteristic of the C=O stretching vibration of carboxyl
348 and acetyl moieties in hemicelluloses (xyloglucan) [25], decreases as well as that of the peak at
349 1243 cm⁻¹, which corresponds to the C-O linkage, as found in guaiacyl aromatic methoxyl and
350 acetyl moieties of xyloglucan [25]. On the other hand, the peaks at 2920 and 2850 cm⁻¹
351 corresponding to the C-H stretching of lignin and cellulose [26,27] become more evident.



352
 353 **Fig. 7.** ATR-FTIR spectra of: (a) HF, and (b) HF_{Na} fibres. (1-column fitting image)

354
 355 No great differences in the crystalline structure as well as in the crystallinity index (*CI*) were found
 356 before and after the mild alkali treatment of hemp fibres used here. Indeed, both diffractograms
 357 (Fig. 8) show the four XRD reflections typical of cellulose I at 15, 16.4, 22.6, and 34.3° 2 θ
 358 corresponding, respectively, to (101), (10-1), (002), and (040) crystallographic planes [28,29].
 359 By peak deconvolution a *CI* value of 85% was calculated for HFs and of 87% for HF_{Na}s, that is a
 360 slightly higher value, also considering the experimental error intrinsic to the technique. However, it
 361 is worth mentioning that the fibre crystallinity index is generally used for comparison purpose
 362 before and after different treatments rather than to evaluate absolute crystallinity [30-32]. Moreover,
 363 the two peaks at 15 and 16.5° appeared partially overlapped, indicating that the HF_{Na} fibres still
 364 contain a certain amount of amorphous material [33], as expected following a mild alkali treatment
 365 as in the present case; when these two peaks are well separated and pronounced the fibres contain
 366 higher amounts of crystalline cellulose.

367



368

369 **Fig. 8.** XRD diffractograms of: (a) HF and HF_{Na} fibres, and (b) example of peak deconvolution of
 370 the XRD pattern of HFs. (1-column fitting image)

371

372 **Thermal and** thermo-oxidative stability of hemp fibres before and after the treatment with sodium
 373 hydroxide and the subsequent surface modification with the MCOs (see later in the text) were
 374 investigated by TGA analysis in dynamic mode. Relevant **TGA data collected are summarized in**
 375 Table 3. The fibre treatment with NaOH slightly increases the temperature at which the fibres start
 376 to degrade **under O₂ atmosphere**; indeed, **T₅ values of HF_{Na}s is about 10 higher than that of HFs.**
 377 This can be explained by the partial removal of non-cellulosic and amorphous cellulose components
 378 (which decompose at lower temperatures) with consequent slight increase in crystallinity. **Both**
 379 **under O₂ and N₂ atmosphere, the T_{vmax} values before and after NaOH treatment are quite similar.**

380

381 **Table 3.** Water content at 150°C and T_5 and T_{Vmax} decomposition temperatures of hemp fibres
 382 determined by TGA.

Sample	H ₂ O content @ 150°C (wt.%)	Under O ₂		Under N ₂
		T_5 (°C)	T_{Vmax} (°C)	T_{Vmax} (°C)
HF _s	2.2	307	358	374
HF _{NaS}	2.5	315	355	371
HF _{Na} -C-pMCOs	1.7	327	368	-
HF _{Na} -npMCOs	1.8	325	369	378

383

384 The surface modification of HF_{NaS} with the synthesized MCOs could in principle be accomplished
 385 through different procedures:

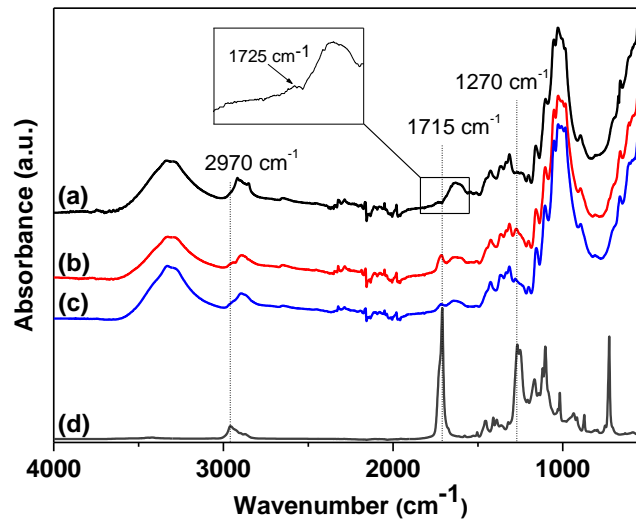
- 386 (i) adsorption of the MCOs onto HF_{NaS} followed by ED-ROP directly during mixing with PBAT
 387 in internal mixer;
- 388 (ii) adsorption of non-purified npMCOs, i.e. the crude MCOs as obtained from CDP still
 389 containing the transesterification catalyst, and their subsequent ED-ROP onto HF_{NaS} prior to
 390 incorporation of the so-modified fibres into the PBAT matrix;
- 391 (iii) previous anchorage of the transesterification catalyst onto HF_{NaS}, subsequent adsorption of
 392 purified pMCOs, that is cleaned by catalyst through elution on Al₂O₃, and ED-ROP prior to
 393 fibres incorporation in the PBAT matrix.

394 The easiest and fastest strategy (i) unfortunately gave composite materials with no appreciable
 395 improvement in their final properties [17]; this could be ascribed to uncontrolled ED-ROP
 396 conditions and too short residence times in the mixer. As a consequence, (ii) and (iii)
 397 compatibilization strategies appeared more promising and were further investigated.

398 As detailed in the Materials and methods section, two procedures for modification of HF_{NaS} with the
 399 MCOs, respectively starting from npMCOs or pMCOs macrocycles, were followed. The ED-ROP
 400 of the MCOs adsorbed onto the hemp fibres was performed by using the reaction conditions
 401 (190°C, 30 min) established by the polymerization experiments previously carried out in the DSC
 402 pan. The two MCO-modified fibre samples obtained after ED-ROP and extraction of unreacted or
 403 ungrafted products were called HF_{Na}-npMCOs and HF_{Na}-C-pMCOs, respectively.

404 The presence of PBAT oligomers (M_p ranging from 5000 to 7000 g/mol) in the soluble fractions
 405 obtained by washing both MCO-modified fibre samples with CHCl₃ was ascertained by FTIR and
 406 SEC analyses. This finding confirms that unreacted macrocycles and/or ungrafted linear oligomers
 407 were effectively removed from hemp fibres. As a consequence, the reacted portion which remains
 408 on the fibres is actually grafted. The ATR-FTIR analysis of fibres modified by both procedures (ii)
 409 and (iii) featured the presence on their surface of the PBAT moieties, as desired. In particular, the

410 peaks at 1715 and 1270 cm^{-1} , respectively due to the stretching modes of C=O and C-O of the ester
411 linkages belonging to the polyester chains, were observed (Fig. 9). It is worth noticing that these
412 peaks are absent in the spectrum of alkali treated HF_{NaS} , that only exhibits a feeble signal ascribable
413 to carbonyl groups centred at 1735 cm^{-1} .
414



415
416 **Fig. 9.** ATR-FTIR spectra of: (a) HF_{NaS} , (b) $\text{HF}_{\text{Na-npMCOs}}$, (c) $\text{HF}_{\text{Na-C-pMCOs}}$, and (d) PBAT.
417 **Inset shows the ATR-FTIR spectrum of HF_{NaS} in the 1950-1550 cm^{-1} window.** (1-column fitting
418 image)

419
420 As shown by the parameters collected in Table 3, the surface modification of HF_{NaS} with the MCOs
421 results in an improvement of the thermo-oxidative stability of the fibres. Moreover, the water
422 content of fibres stored in an ambient environment ($T \approx 25^\circ\text{C}$, $\text{RH} \approx 65\%$), evaluated as the weight
423 loss at 150°C , decreases after modification with the MCOs, indicating, as expected, a reduction of
424 the surface hydrophilicity.

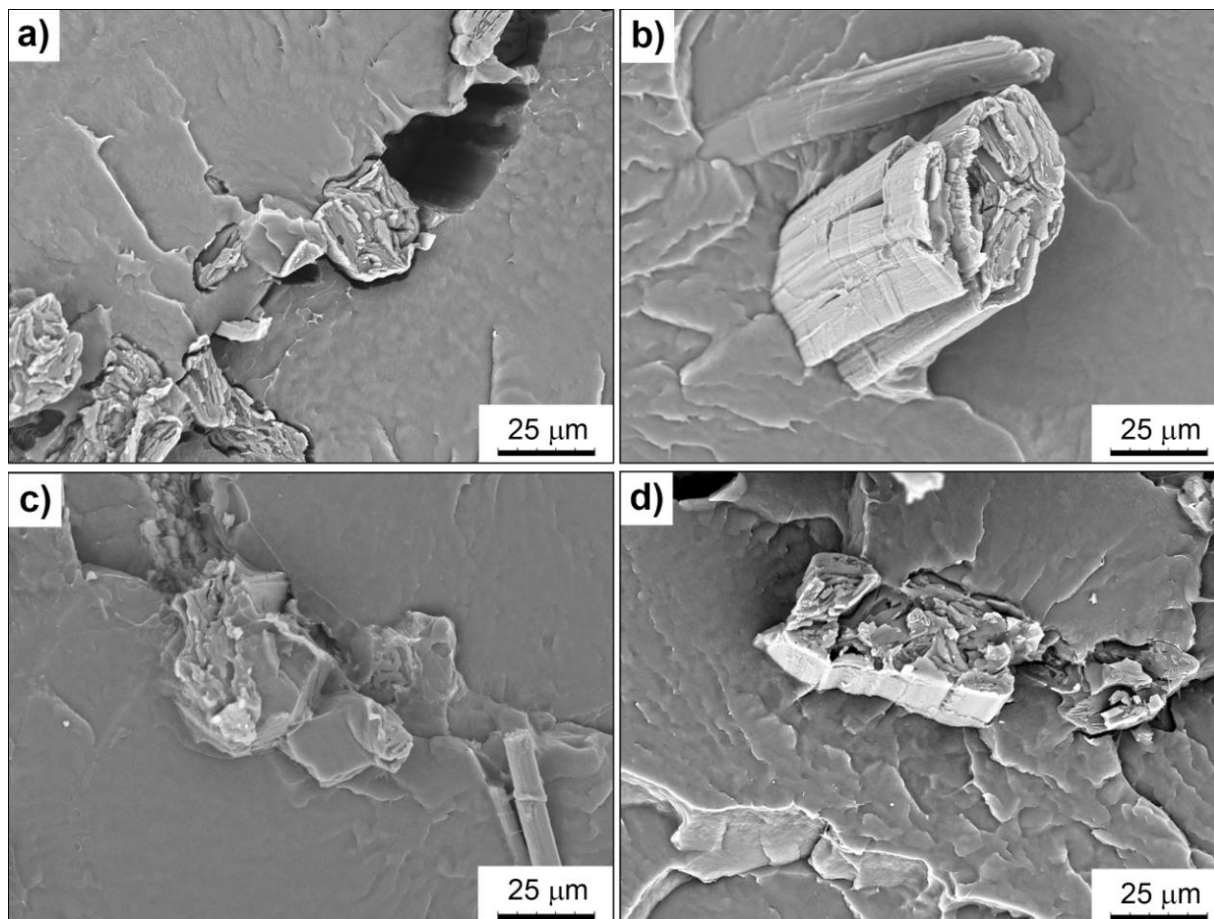
425 SEM images of Fig. 6 c,d clearly show the presence of a polymeric layer covering the surface of
426 fibres modified with npMCOs. The increase in thermo-oxidative stability of both samples of MCO-
427 modified fibres can be ascribed to the protection exerted by this polymeric layer, being the thermo-
428 oxidative decomposition temperatures T_5 and T_{Vmax} recorded for PBAT in the same conditions,
429 respectively 344 and 415°C .

430 431 3.4. PBAT/hemp fibres eco-composites

432 In order to evaluate the effect of the fibre modification on the fibre-polymer adhesion, preliminary
433 tests of adhesion were carried out on composites containing < 5 wt.% of HF, HF_{Na} , $\text{HF}_{\text{Na-npMCO}}$
434 or $\text{HF}_{\text{Na-C-pMCO}}$ fibres prepared by placing slightly stretched fibres between two sheets of PBAT

435 (previously obtained by compression moulding of PBAT pellets) and by moulding the resulting
436 “sandwich” in the hot-press, as detailed in the Materials and methods section.

437 The ensuing samples were then fractured in liquid nitrogen and the morphological characterization
438 of their fractured surfaces was performed by SEM. Some representative images taken at the same
439 magnification were shown in Fig. 10.



440
441 **Fig. 10.** SEM micrographs of preliminary PBAT-based composites containing < 5 wt.% of: (a)
442 uncut HF, (b) HF_{Na}, (c) HF_{Na}-npMCO, and (d) HF_{Na}-C-pMCO fibres. (2-column fitting image)

443
444 Untreated HFs resulted very poorly adhered to the PBAT matrix (Fig. 10a). As shown in Fig. 10b,
445 while the pre-treatment with NaOH improved fibre/matrix adhesion. The adhesion of the fibres to
446 the PBAT matrix was noticeably further enhanced when HF_{Na}-npMCOs (Fig. 10c) or HF_{Na}-C-
447 pMCOs (Fig. 10d) were used. No appreciable differences were evidenced between the two samples
448 containing the fibres modified with the MCOs. This suggests that the macrocycles purification step
449 and the subsequent addition of the catalyst prior to ED-ROP can be avoided, using directly the non-
450 purified macrocycles as the compatibilizing agent.

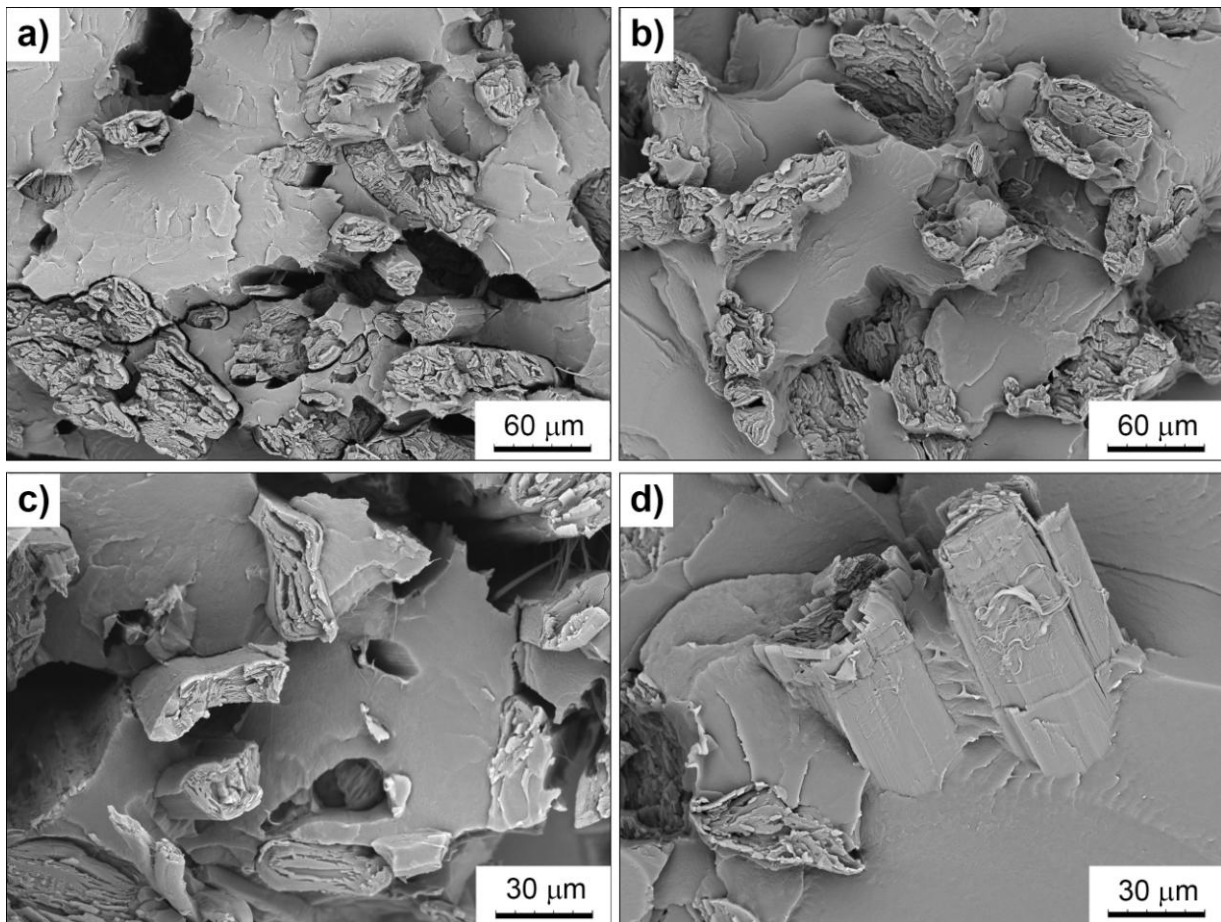
451 On the basis of these preliminary results, PBAT-based composites containing higher amounts
452 (about 40 wt.%) of uncut oriented HF, HF_{Na}, and HF_{Na}-npMCO fibres were prepared by

453 compression moulding through the two-steps method described in the Materials and methods
454 section.

455 The ensuing eco-composites were then characterized by SEM microscopy to estimate fibre-matrix
456 interaction and by performing uniaxial tensile tests to evaluate their mechanical properties.

457 SEM micrographs of Fig. 11 confirm the higher interaction of MCO-modified fibres (Fig. 11 b,d)
458 with the PBAT matrix if compared to the poor one shown by untreated HF fibres (Fig. 11 a,c).

459



460

461 **Fig. 11.** SEM micrographs of PBAT-based composites containing: (a,c) uncut HF, and (b,d) HF_{Na}-
462 npMCO fibres. (2-column fitting image)

463

464 **Thermal stability of PBAT, HF fibres, and HF-PBAT composites was investigated by TGA analysis**
465 **carried out in dynamic mode under nitrogen; the characteristic temperatures are reported in Table 4.**
466 **A double step weight loss was observed in the TG curve of PBAT-based composites: the first step,**
467 **between 300 and 400°C, corresponds to the thermal degradation of the hemp fibres (T_{onset1} and**
468 **T_{Vmax1}), and the second one, in the range 400-500°C, is ascribable to the thermal degradation of the**
469 **PBAT matrix (T_{onset2} and T_{Vmax2}). The degradation onset of the hemp fibres (about 340°C) was**
470 **shifted toward higher temperatures (about 360°C) by their incorporation into the PBAT matrix.**

471 On the other hand, the thermal degradation of the PBAT (T_{onset2}) in the composites is practically
 472 independent on the fibre added and slightly lower than that of neat PBAT.

473

474 **Table 4.** T_{onset} and T_{Vmax} decomposition temperatures of hemp fibres, neat PBAT, and PBAT/hemp
 475 fibres eco-composites determined by TGA at 10°C/min under N₂.

Sample	T_{onset1} (°C)	T_{Vmax1} (°C)	T_{onset2} (°C)	T_{Vmax2} (°C)
PBAT	-	-	385	418
PBAT + HF	361	384	372	422
PBAT + HF_{Na}	353	378	375	425
PBAT + HF_{Na}-npMCO	357	384	362	419

476

477 The mechanical properties of these PBAT-based composites were evaluated by uniaxial tensile
 478 tests; the results (Table 5) were normalized with respect to the effective amount of fibres in the
 479 composite sample, as determined by TGA. The presence of the fibres resulted in a great increase in
 480 storage modulus (E) and stress at break (σ_b) values when compared to those of the neat PBAT.
 481 Correspondingly, the composite samples are more brittle, as evidenced by the remarkable reduction
 482 of the elongation at break (ε_b).

483

484 **Table 5.** Tensile modulus (E), stress (σ_b) and strain (ε_b) at break obtained for neat PBAT and
 485 PBAT-based composites containing about 40 wt.% hemp fibres.

Sample	E (MPa)	σ_b (MPa)	ε_b (%)
PBAT	75 ± 8	24 ± 2	1527 ± 86
PBAT + HF	2435 ± 249	111 ± 14	12 ± 1
PBAT + HF_{Na}	4805 ± 550	97 ± 12	4 ± 1
PBAT + HF_{Na}-npMCO	5480 ± 280	76 ± 14	2 ± 0.3

486

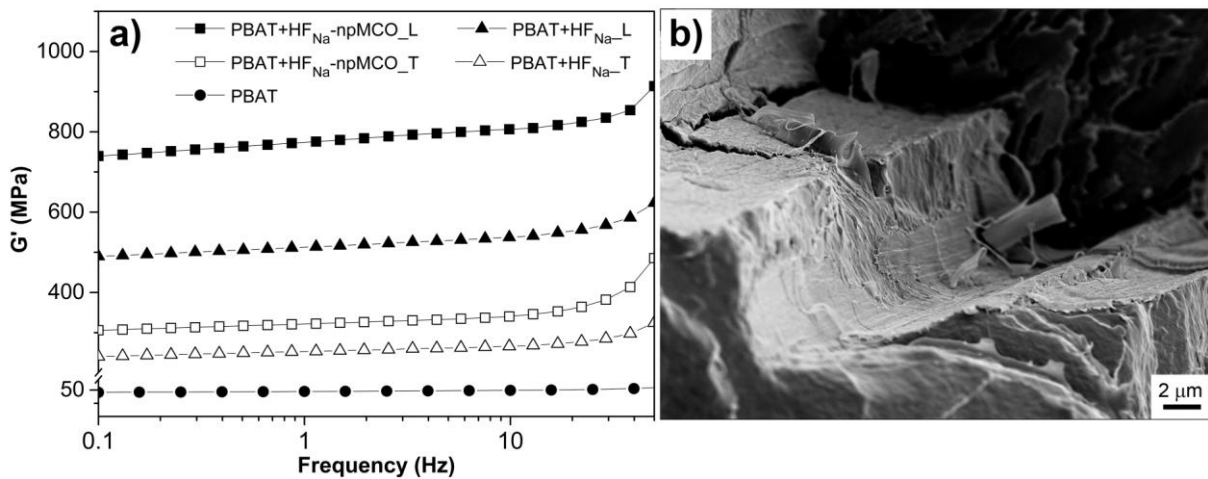
487 Among the composites, the sample containing the MCO-modified fibres (**PBAT + HF_{Na}-npMCO**)
 488 revealed the highest E value, indicative of the beneficial effect of such modification on the fibre-
 489 matrix adhesion, which in turn promotes under loading an efficient stress transfer from matrix to the
 490 fibrous reinforcement. The slight decrease of the stress at break could be ascribed to a mechanical
 491 weakening of the hemp fibres due to the thermal treatment carried out during the ED-ROP reaction
 492 (190°C, 30 min). Even though a TGA isothermal analysis carried out at 200°C in O₂ atmosphere for

493 30 min revealed a good thermo-oxidative resistance of HF_{Na}s fibres (the weight loss is about 0.5%),
494 the maintenance at high temperature in oxidative atmosphere could be slightly detrimental to the
495 mechanical properties of the fibres, as reported by Prasad *et al.* [34].

496 Dynamic-mechanical analysis (DMA) of PBAT and PBAT-based composites containing HF_{Na} and
497 HF_{Na}-npMCO fibres was carried out to evaluate the effective reinforcement exerted by the fibres in
498 terms of elastic or storage modulus (G'). The resulting curves are shown in Fig. 12a. The presence
499 of the long fibres in the composites resulted in a strong increase of the mechanical properties with
500 respect to those of the neat PBAT (G' at 1Hz = 47 MPa). As expected, this effect is more
501 pronounced along the fibre axis than in the orthogonal direction: in fact, the values of G' measured
502 at 1Hz are respectively 510 and 260 MPa for the PBAT + HF_{Na} composite, and the corresponding
503 values for PBAT + HF_{Na}-npMCO are 770 and 320 MPa. The beneficial effect of the MCO-
504 functionalization of HFs with respect to the simple alkali treatment is evidenced by an increase in
505 G' of the 51% in the longitudinal direction and 23% in the transversal one.

506 The effectiveness of the compatibilization through MCOs is also visible in the FE-SEM micrograph
507 of the PBAT + HF_{Na}-npMCO sample taken after DMA analysis and reported in Fig. 12b. Besides
508 fibres detached from the matrix, as a consequence of the torsional strain, the fibre external layer
509 remain adhered to the polymer, indicating the good adhesion between the HF-modified surface and
510 the PBAT matrix.

511



512
513 **Fig. 12.** (a) DMA curves of PBAT, PBAT + HF_{Na} and PBAT + HF_{Na}-npMCO samples obtained in
514 longitudinal (L) and transversal (T) directions; (b) FE-SEM micrograph of PBAT + HF_{Na}-npMCO
515 sample after DMA analysis. (2-column fitting image)

516

517

518

519 **4. Conclusions**

520 CDP of poly(1,4-butylene adipate-*co*-terephthalate) (PBAT) was, for the first time, successfully
521 performed at high dilution, in mild conditions and in the presence of a suitable transesterification
522 catalyst, achieving quantitative yields of the corresponding macrocyclic oligomers (MCOs).

523 The reconversion of the MCOs into linear polymeric chains was successfully accomplished by ED-
524 ROP, carried out by simply heating the neat macrocycles as obtained from CDP, without any
525 further addition of catalyst.

526 ED-ROP of the MCOs adsorbed onto hemp fibres previously mildly treated with aqueous NaOH
527 to remove non-cellulosic and amorphous components and favour accessibility to the functional
528 groups, led to modified fibres with anchored PBAT oligomers, that is to a perfectly suited
529 compatibilizing agent for PBAT composites reinforced with hemp fibres.

530 PBAT-based composites containing about 40 wt.% of pristine, NaOH-treated, and MCO-modified
531 hemp fibres were prepared by compression moulding. The sample compatibilized with the MCO-
532 modified fibres showed the best fibre/matrix adhesion, which resulted in enhanced mechanical
533 properties in terms of elastic modulus with respect to not only the neat PBAT but also to the other
534 composites.

535 The overall results gathered so far validate the compatibilization strategy adopted for preparing eco-
536 friendly composite materials based on a biodegradable polyester matrix reinforced with high
537 amounts of low cost fibres arising from hemp manufacturing by-products.

538

539

540 **Acknowledgements**

541 Dr. F. Giunco (CNR-ISMAL Genova) for helpful contribution, Mr. M. Canetti (CNR-ISMAL
542 Milano) for WAXD measurements.

543

544 This research did not receive any specific grant from funding agencies in the public, commercial, or
545 not-for-profit sectors.

546

547

548 **References**

549 [1] P. Hodge, Entropically driven ring-opening polymerization of strainless organic macrocycles,
550 Chem. Rev. 114 (2014) 2278-2312.

551 [2] P. Hodge, Recycling of condensation polymers via ring-chain equilibria, Polym. Adv. Technol.
552 26 (2015) 797-803.

- 553 [3] L. Conzatti, R. Utzeri, P. Hodge, P. Stagnaro, A novel tin-based imidazolium-modified
554 montmorillonite catalyst for the preparation of poly(butylene terephthalate)-based nanocomposites
555 using in situ entropically-driven ring-opening polymerization, *RSC Adv.* 5 (2015) 6222-6231.
- 556 [4] P. Hodge, Cyclodepolymerization as a method for the synthesis of macrocyclic oligomers,
557 *React. Funct. Polym.* 80 (2014) 21-32.
- 558 [5] D.J. Brunelle, Macrocycles for the synthesis of high molecular weight polymers, in: J.R. Ebdon,
559 G.C. Eastmond (Eds.), *New methods of polymer synthesis - vol. 2*, Blackie, London, 1995, pp. 197-
560 235.
- 561 [6] A. Ben-Haida, H.M. Colquhoun, P. Hodge, J.L. Stanford, A novel approach to processing high-
562 performance polymers that exploits entropically-driven ring-opening polymerization, *Macromol.*
563 *Rapid Comm.* 26 (2005) 1377-1382.
- 564 [7] M. Alessi, L. Conzatti, P. Hodge, S. Tagliatalata Scafati, P. Stagnaro, A possible means to assist
565 the processing of PET, PTT and PBT, *Macromol. Mater. Eng.* 295 (2010) 374-380.
- 566 [8] M.N. Belgacem, A. Gandini, *Monomers, polymers and composites from renewable resources*,
567 Elsevier, Oxford UK, 2008.
- 568 [9] O. Faruk, A.K. Bledzki, H.P. Fink, M. Sain, *Biocomposites reinforced with natural fibers: 2000-*
569 *2010*, *Prog. Polym. Sci.* 37 (2012) 1552-1596.
- 570 [10] M.P.M. Dicker, A.B. Baker, P.F. Duckworth, A.B. Baker, G. Francois, M.K. Hazzard, P.M.
571 Weaver, *Green composites: A review of material attributes and complementary applications*,
572 *Compos. Part A-Appl. S.* 56 (2014) 280-289.
- 573 [11] T. Gurunathan, S. Mohanty, S. K. Nayak, A review of the recent developments in
574 biocomposites based on natural fibres and their application perspectives, *Compos. Part A-Appl. S.*,
575 77 (2015) 1-25.
- 576 [12] K. L. Pickering, M. G. Aruan Efendy, T. M. Le, A review of recent developments in natural
577 fibre composites and their mechanical performance, *Compos. Part A-Appl. S.* 83 (2016) 98-112.
- 578 [13] S. Kalia, B.S. Kaith, I. Kaur, Pretreatments of natural fibers and their application as reinforcing
579 material in polymer composites - A review, *Polym. Eng. Sci.*, 49 (2009) 1253-1272.
- 580 [14] L. Conzatti, F. Giunco, P. Stagnaro, M. Capobianco, M. Castellano, E. Marsano, Polyester-
581 based biocomposites containing wool fibres, *Compos. Part A-Appl. S.* 43 (2012) 1113-1119.
- 582 [15] L. Conzatti, F. Giunco, P. Stagnaro, A. Patrucco, C. Marano, M. Rink, E. Marsano,
583 *Composites based on polypropylene and short wool fibres*, *Compos. Part A-Appl. S.* 47 (2013) 165-
584 171.

585 [16] L. Conzatti, F. Giunco, P. Stagnaro, A. Patrucco, C. Tonin, C. Marano, M. Rink, E. Marsano,
586 Wool fibres functionalised with a silane-based coupling agent for reinforced polypropylene
587 composites, *Compos. Part A-Appl. S.* 61 (2014) 51-59.

588 [17] L. Conzatti, R. Utzeri, P. Hodge, P. Stagnaro, Biodegradable polyester-based eco-composites
589 containing hemp fibers modified with macrocyclic oligomers, *AIP Conference Proceedings* 1736,
590 (2016) 020126.

591 [18] L.Y. Mwaikambo, M.P. Ansell, Mechanical properties of alkali treated plant fibres and their
592 potential as reinforcement materials. I. hemp fibres, *J Mater. Sci.* 41 (2006) 2483-2496.

593 [19] L.E. Hult, T. Iversen, J. Sugiyama, Characterization of the supramolecular structure of
594 cellulose in wood pulp fibres, *Cellulose* 10 (2003) 103-110.

595 [20] C.J. Garvey, I.H. Parker, G.P. Simon, On the interpretation of X-ray diffraction powder patterns
596 in terms of the nanostructure of cellulose I fibres. *Macromol. Chem. Phys.* 206 (2005) 1568-1575.

597 [21] S.D. Kamau, P. Hodge, M. Helliwell, Cyclo-depolymerization of poly(propylene
598 terephthalate): Some ring-opening polymerizations of the cyclic oligomers produced, *Polym. Adv.*
599 *Technol.* 14 (2003) 492-501.

600 [22] X. Li, L.G. Tabil, S. Panigrahi, Chemical treatments of natural fiber for use in natural fiber-
601 reinforced composites: A review, *J. Polym. Environ.* 15 (2007) 25-33.

602 [23] R. Agrawal, N.S. Saxena, K.B. Sharma, S. Thomas, M.S. Sreekala, Activation energy and
603 crystallization kinetics of untreated and treated oil palm fibre reinforced phenol formaldehyde
604 composites, *Mat. Sci. Eng. A* 277 (2000) 77-82.

605 [24] T. Fisher, M. Hajaligol, B. Waymack, D. Kellogg, Pyrolysis behavior and kinetics of biomass
606 derived materials, *J. Anal. Appl. Pyrol.* 62 (2002) 331-349.

607 [25] C.M. Popescu, M.C. Popescu, C. Vasile, Structural analysis of photodegraded lime wood by
608 means of FT-IR and 2D IR correlation spectroscopy, *Int. J. Biolog. Macromol.*, 48 (2011) 667-675.

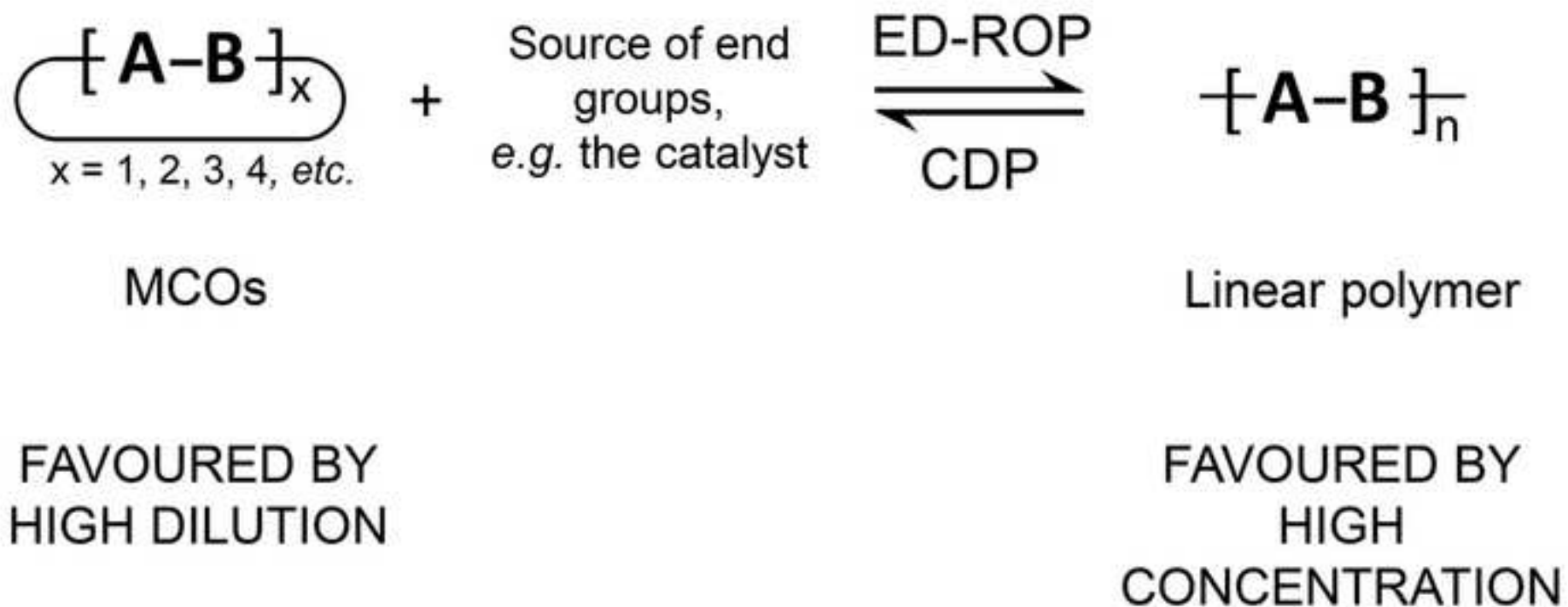
609 [26] K.K. Pandey, A study of chemical structure of soft and hardwood and wood polymers by FTIR
610 spectroscopy, *J. Appl. Polym. Sci.* 71 (1999) 1969-1975.

611 [27] K. Bilba, M.A. Arsene, A. Ouensanga, Study of banana and coconut fibers - Botanical
612 composition, thermal degradation and textural observations, *Biores. Technol.* 98 (2007) 58-68.

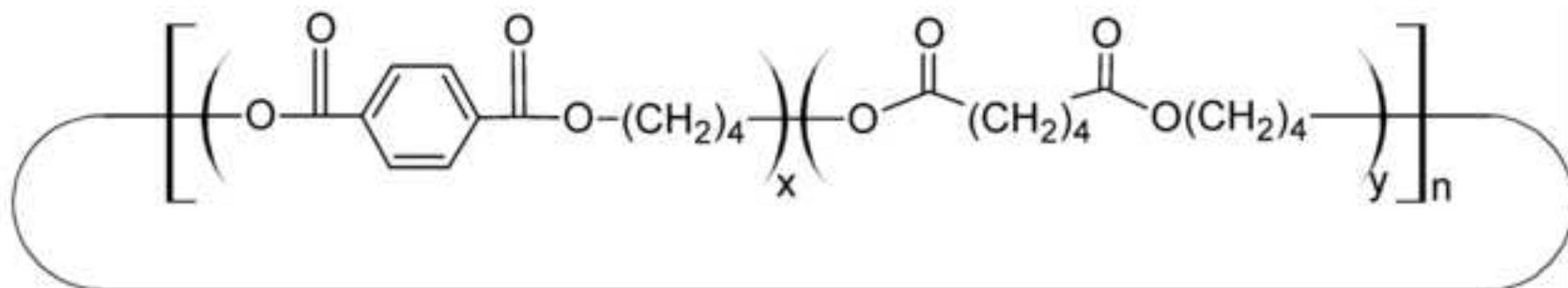
613 [28] C.J. Garvey, I.H. Parker, G.P. Simon, On the interpretation of X-ray diffraction powder
614 patterns in terms of the nanostructure of cellulose I fibres, *Macromol. Chem. Phys.* 206 (2005)
615 1568-1575.

616 [29] S. Park, J.O. Baker, M.E. Himmel, P.A. Parilla, D.K. Johnson, Cellulose crystallinity index:
617 measurement techniques and their impact on interpreting cellulase performance, *Biotechnol.*
618 *Biofuels*, 3 (2010).

- 619 [30] S. Ouajai, R.A., Shanks, Composition, structure and thermal degradation of hemp cellulose
620 after chemical treatments, *Polym. Degrad. Stab.* 89 (2005) 327-335.
- 621 [31] G.W. Beckermann, K.L. Pickering, Engineering and evaluation of hemp fibre reinforced
622 polypropylene composites: Fibre treatment and matrix modification, *Composites: Part A* 39 (2008)
623 979-988.
- 624 [32] M.A. Sawpan, K.L. Pickering, A. Fernyhough, Effect of various chemical treatments on the
625 fibre structure and tensile properties of industrial hemp fibres, *Composites: Part A* 42 (2011) 888-
626 895.
- 627 [33] V. Tserki, N.E. Zafeiropoulos, F. Simon, C. Panayiotou, A study of the effect of acetylation
628 and propionylation surface treatments on natural fibres, *Compos. Part A-Apl. S.* 36 (2005) 1110-
629 1118.
- 630 [34] B. M. Prasad, M. M. Sain, Mechanical properties of thermally treated hemp fibers in inert
631 atmosphere for potential composite reinforcement, *Mat. Res. Innovat.* 7 (2003) 231-238.



MCOs



+
cat.

CDP \rightleftharpoons ED-ROP

PBAT

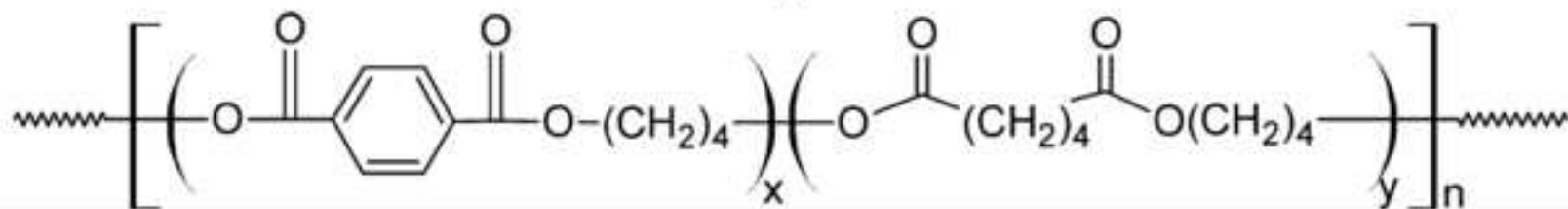


Figure 1
[Click here to download high resolution image](#)

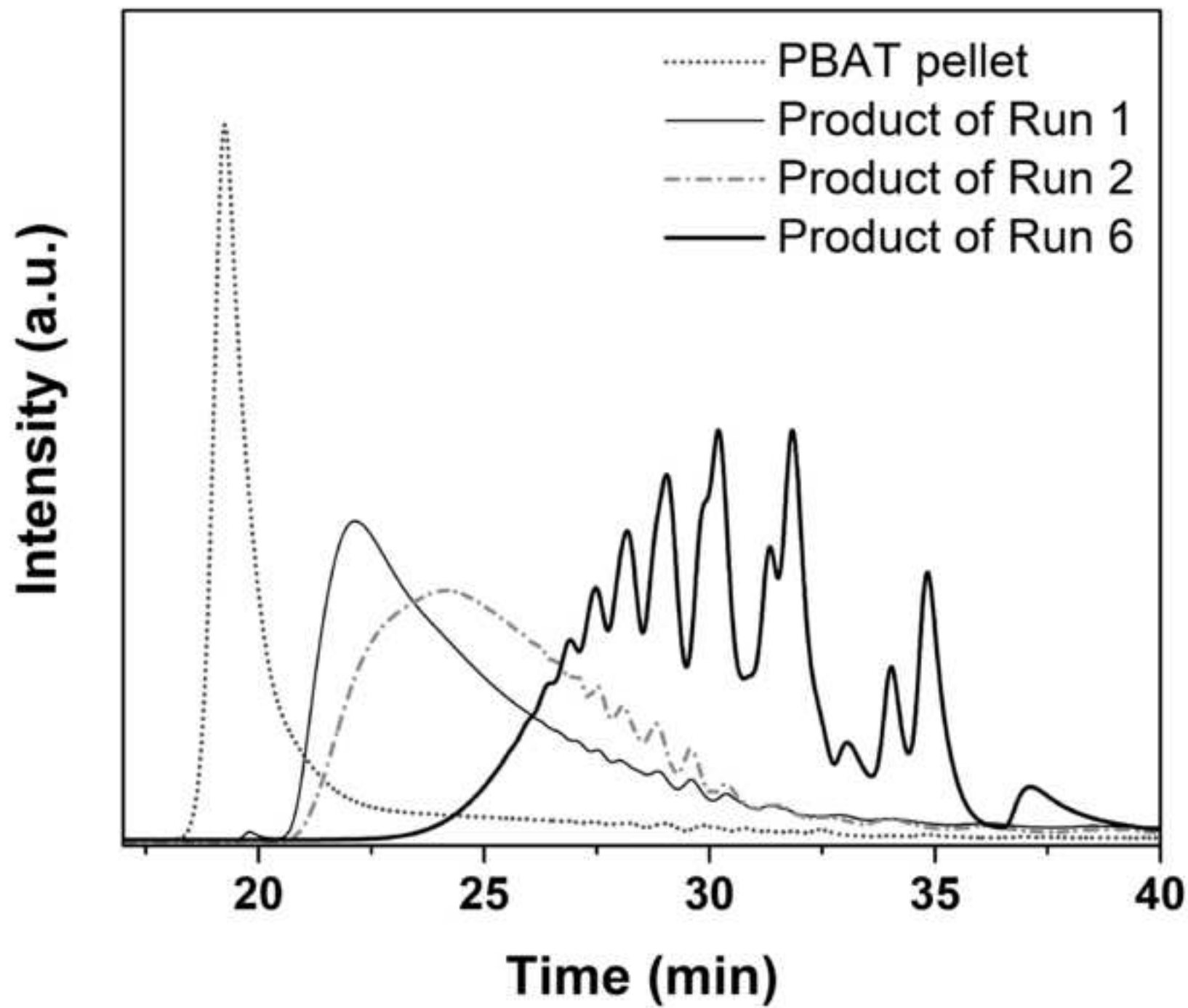


Figure 2
[Click here to download high resolution image](#)

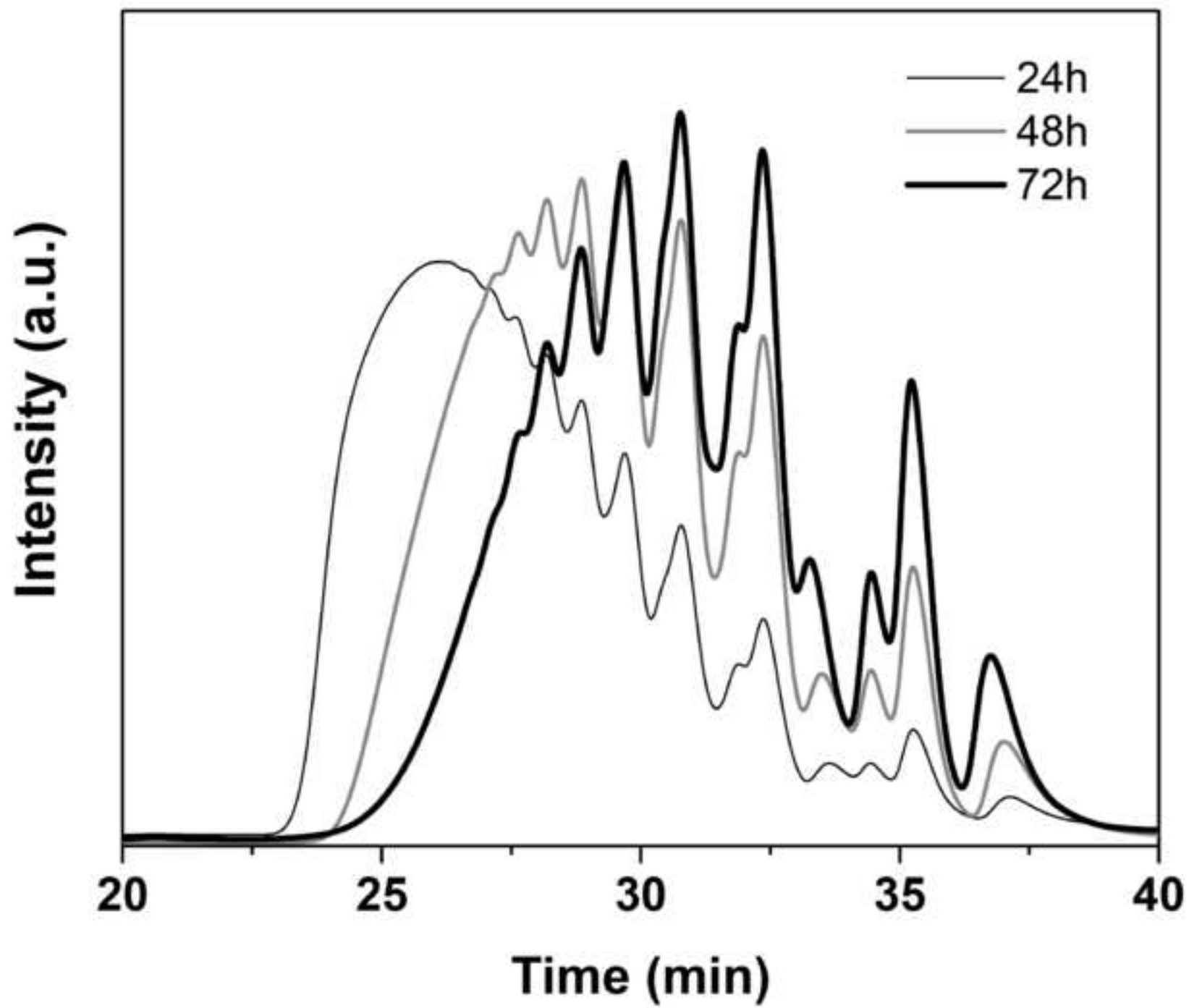


Figure 3
[Click here to download high resolution image](#)

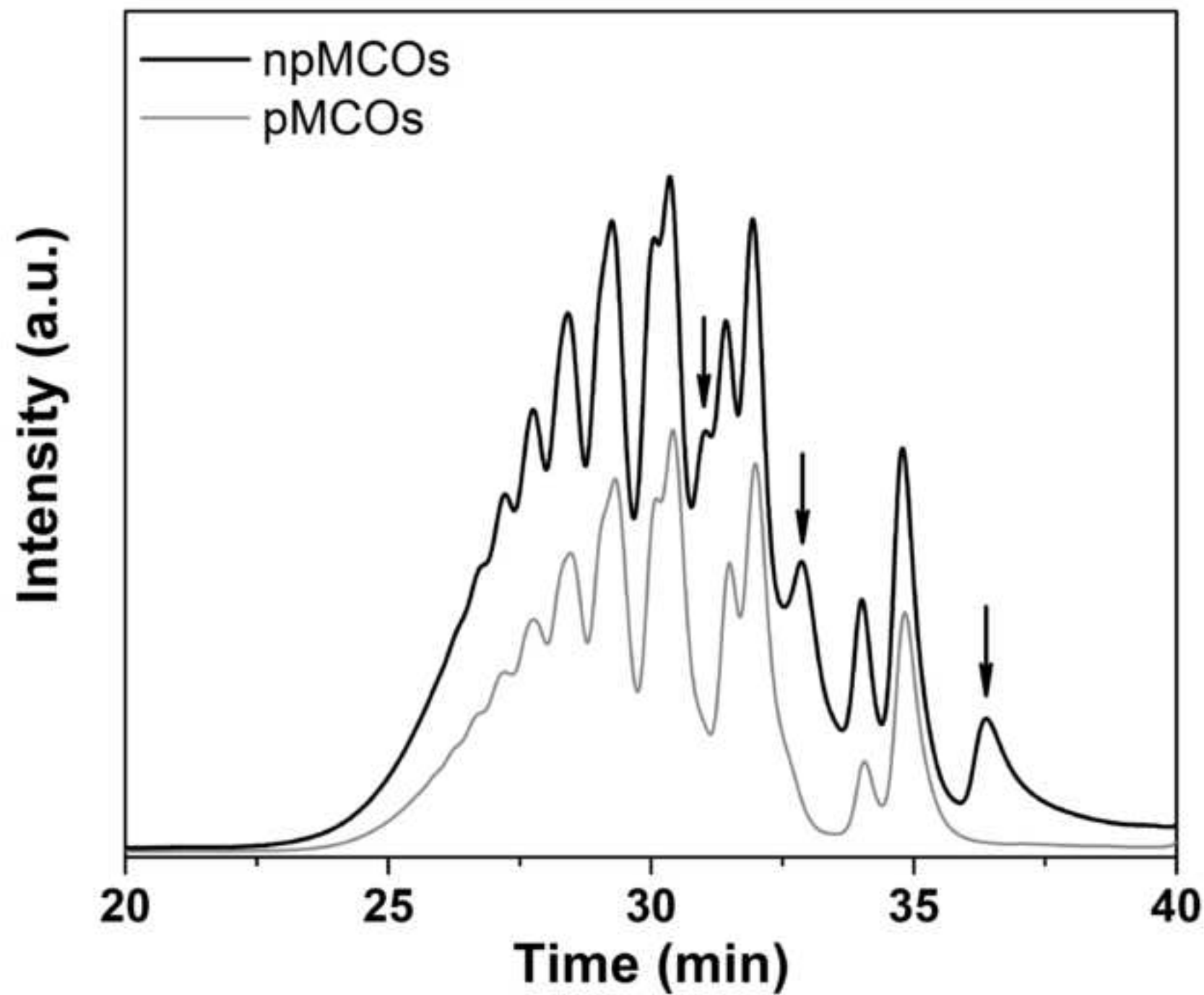


Figure 4

[Click here to download high resolution image](#)

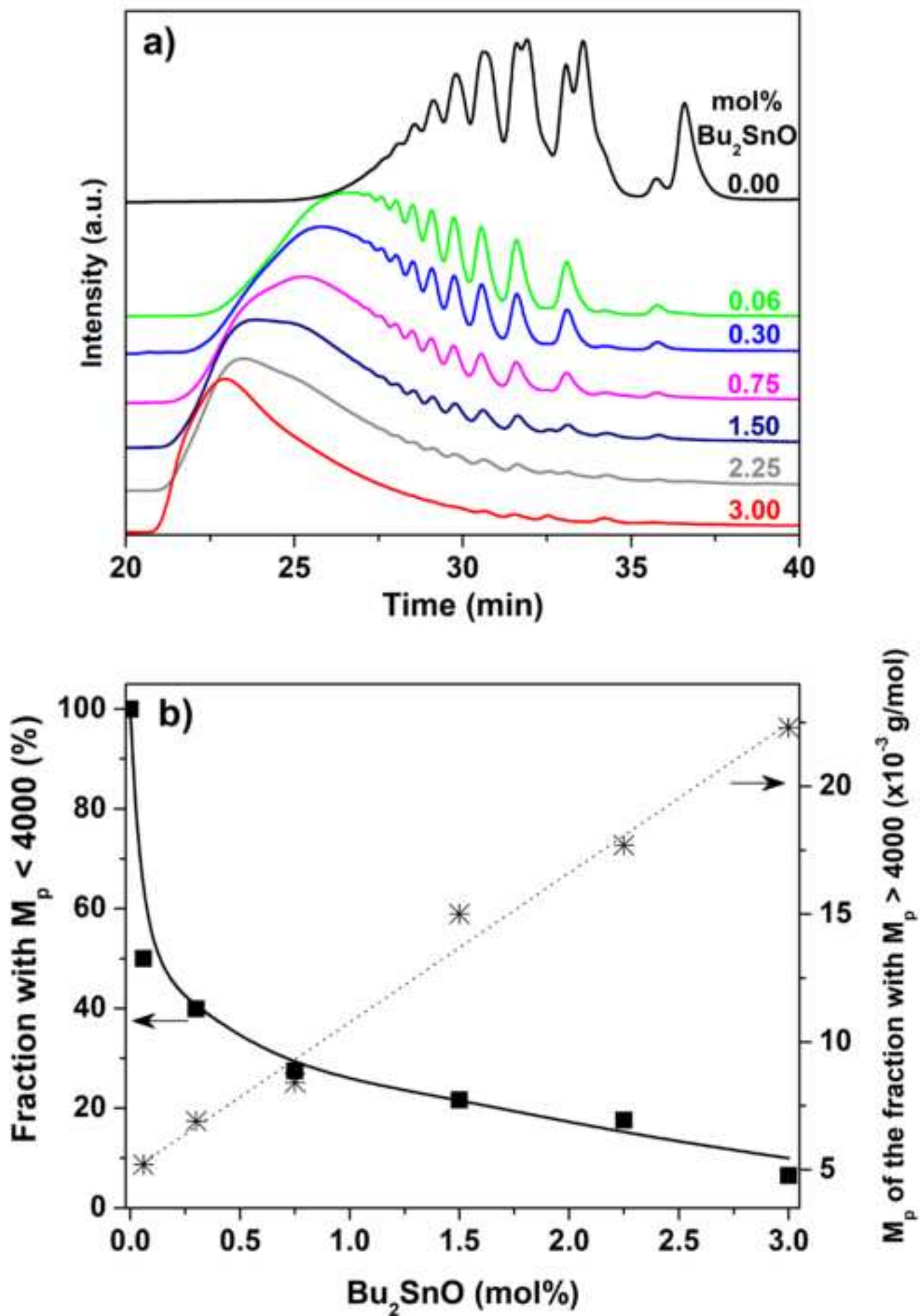


Figure 5

[Click here to download high resolution image](#)

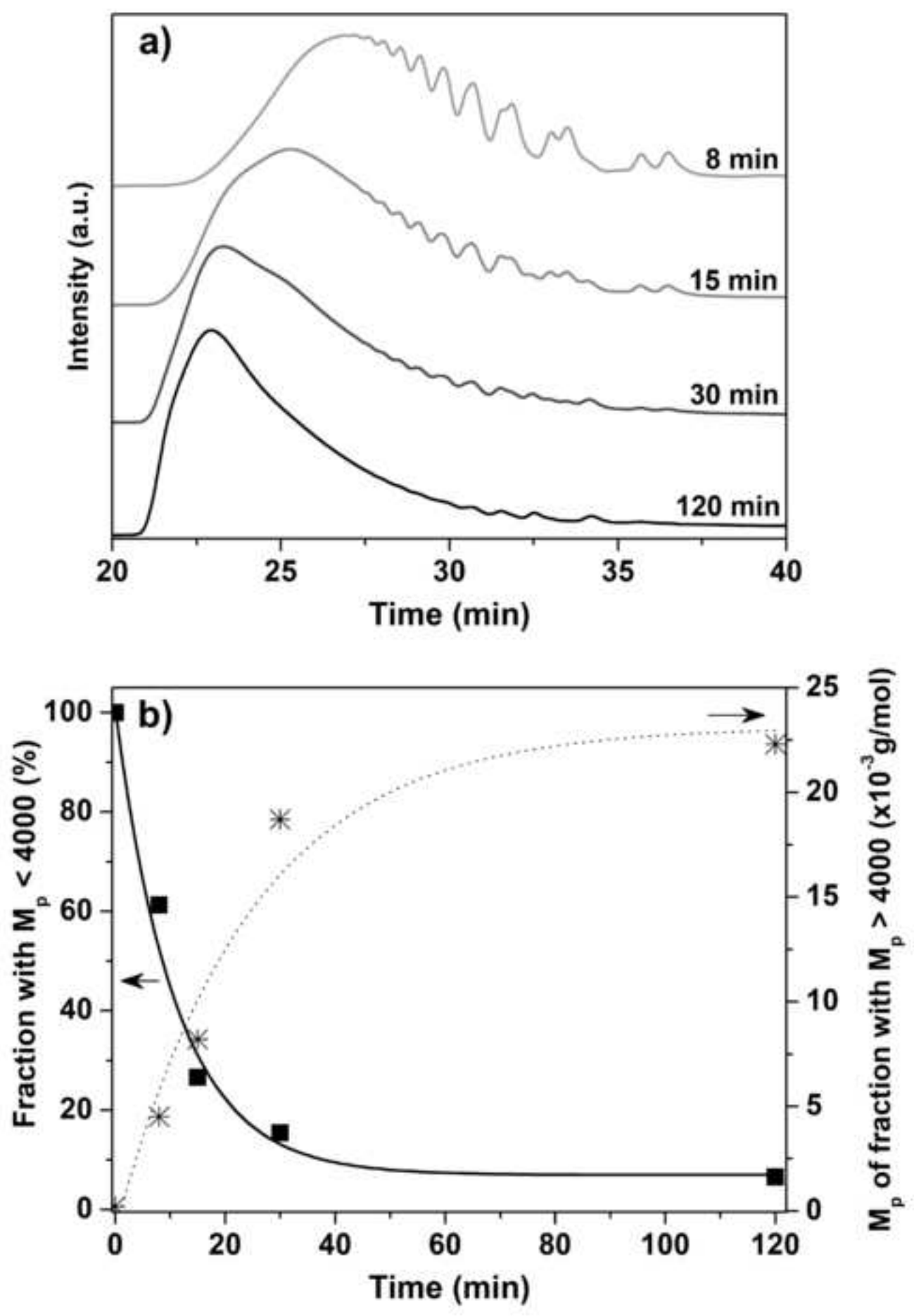


Figure 6
[Click here to download high resolution image](#)

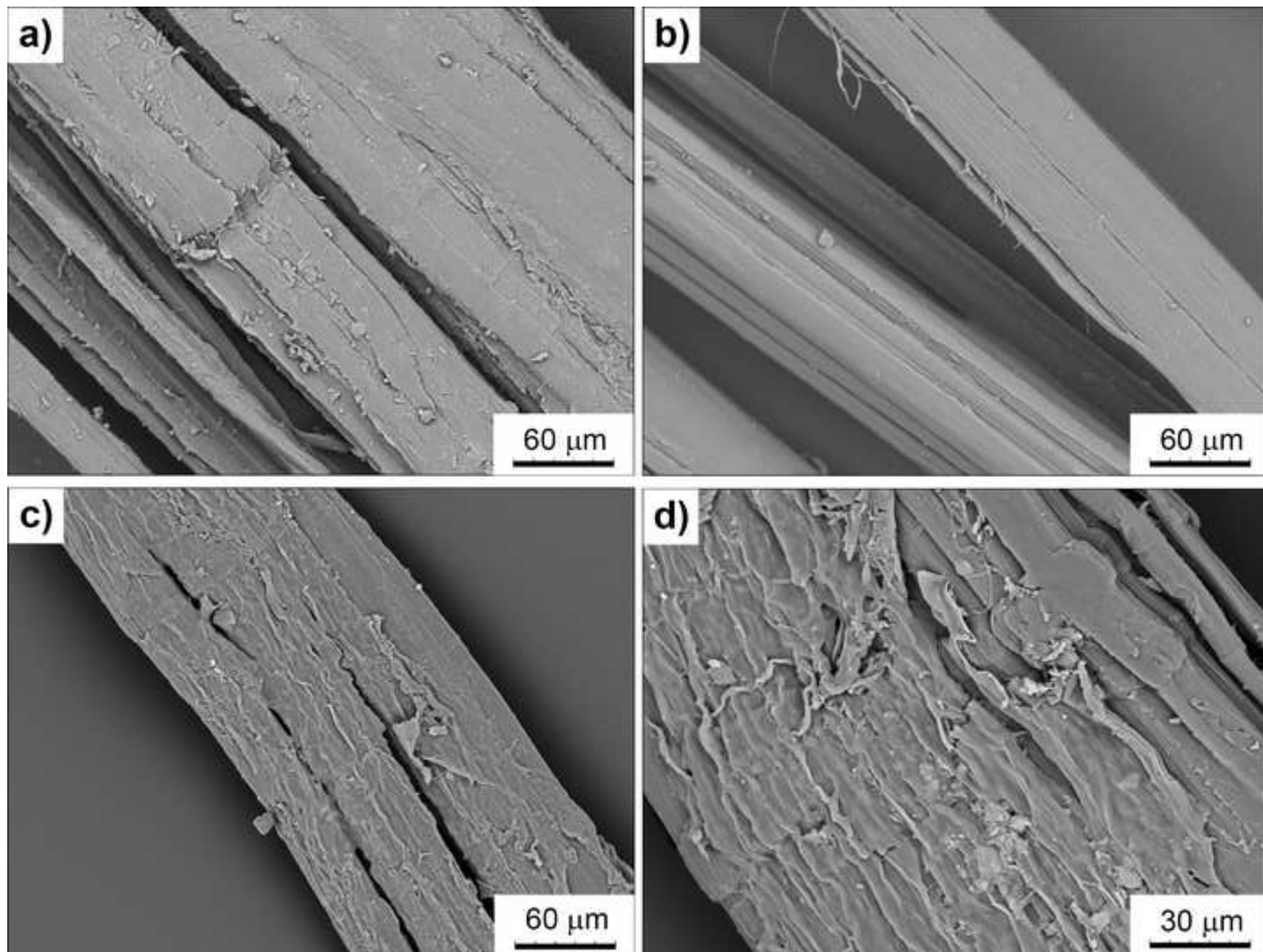


Figure 7
[Click here to download high resolution image](#)

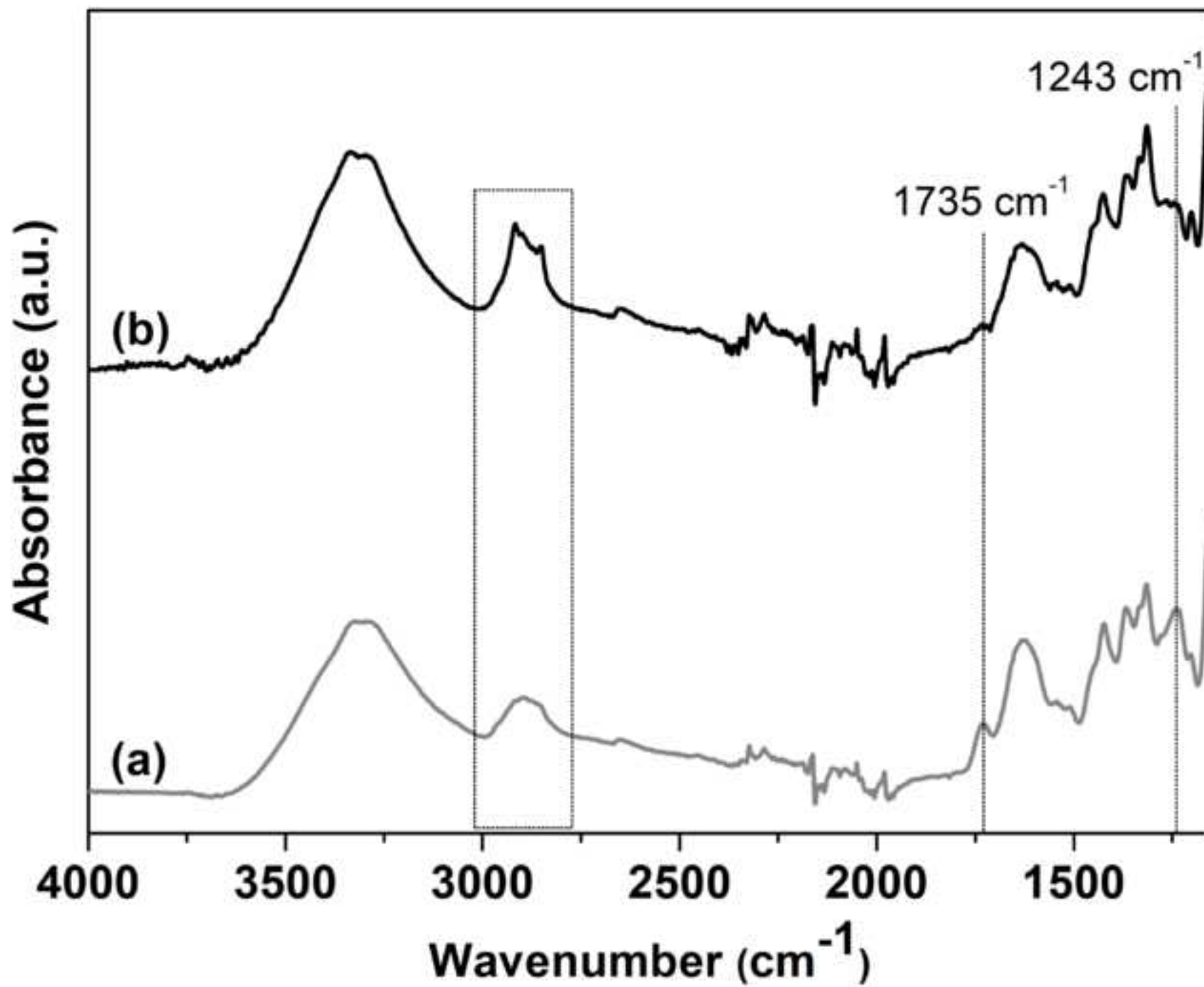


Figure 8

[Click here to download high resolution image](#)

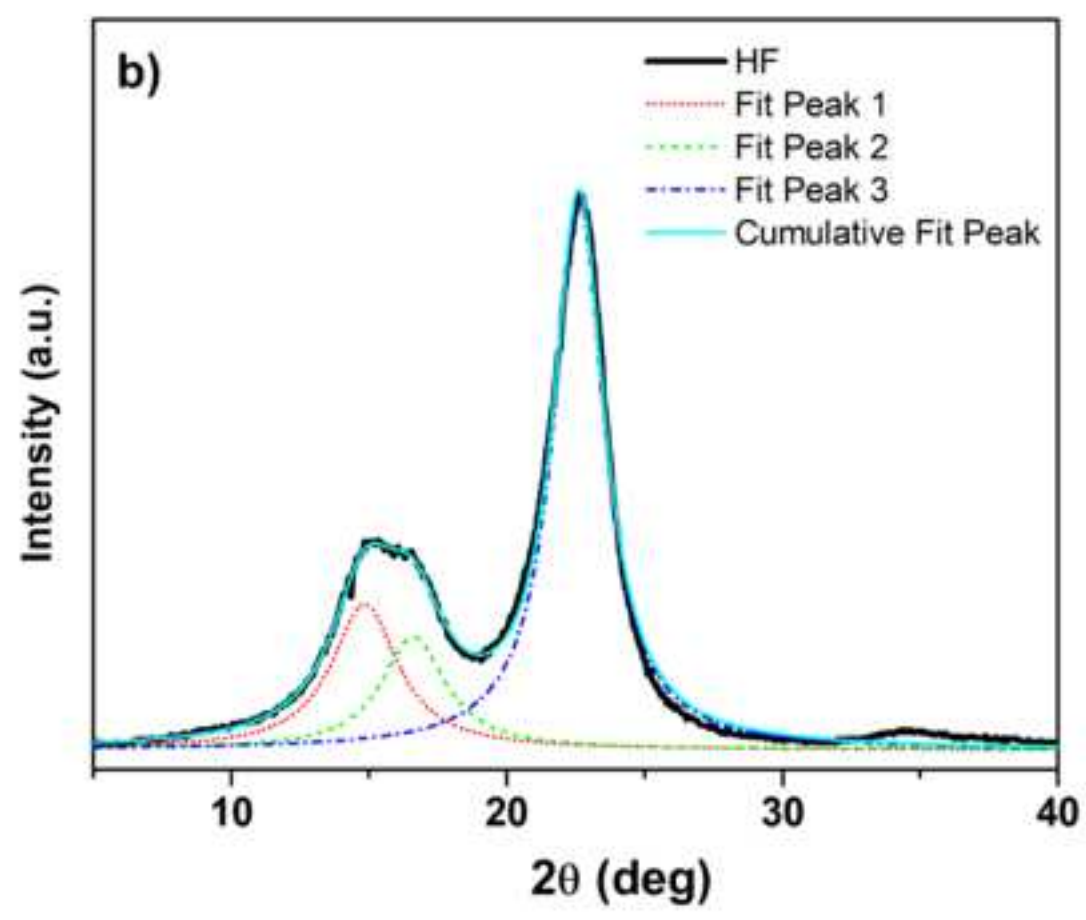
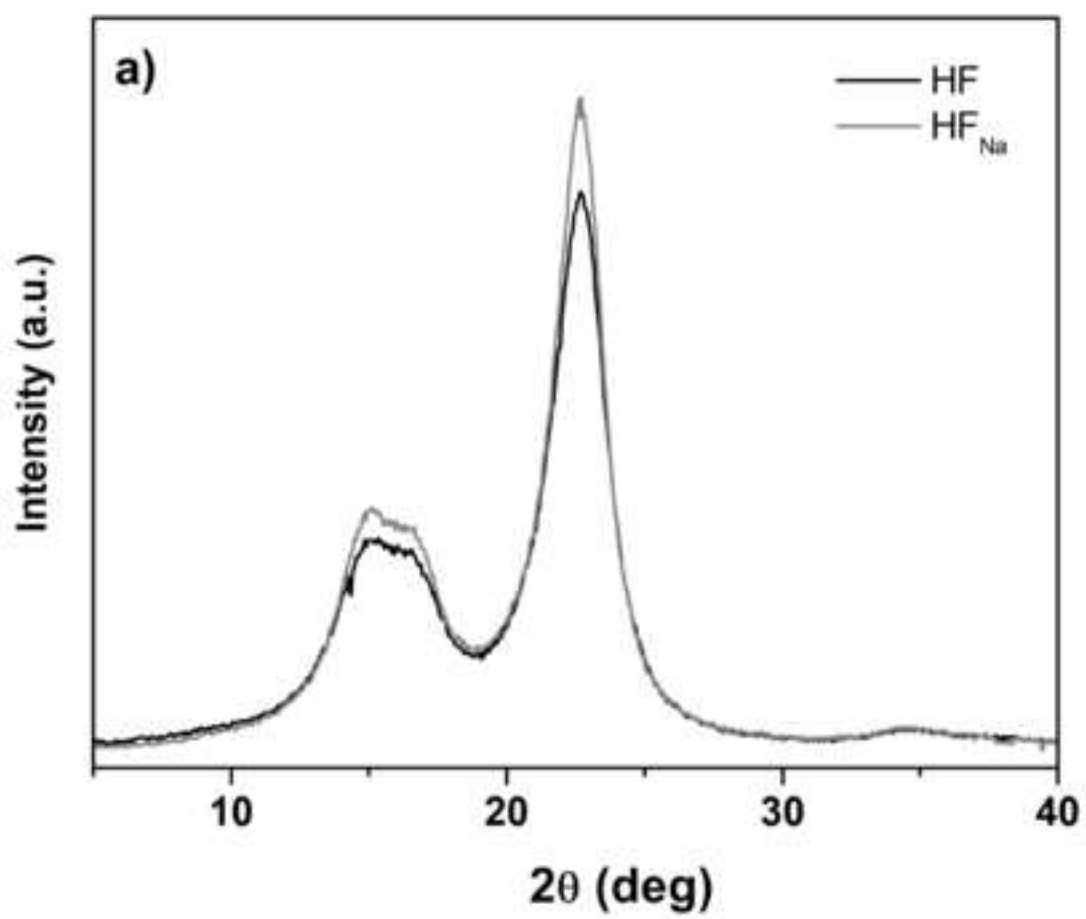


Figure 9
[Click here to download high resolution image](#)

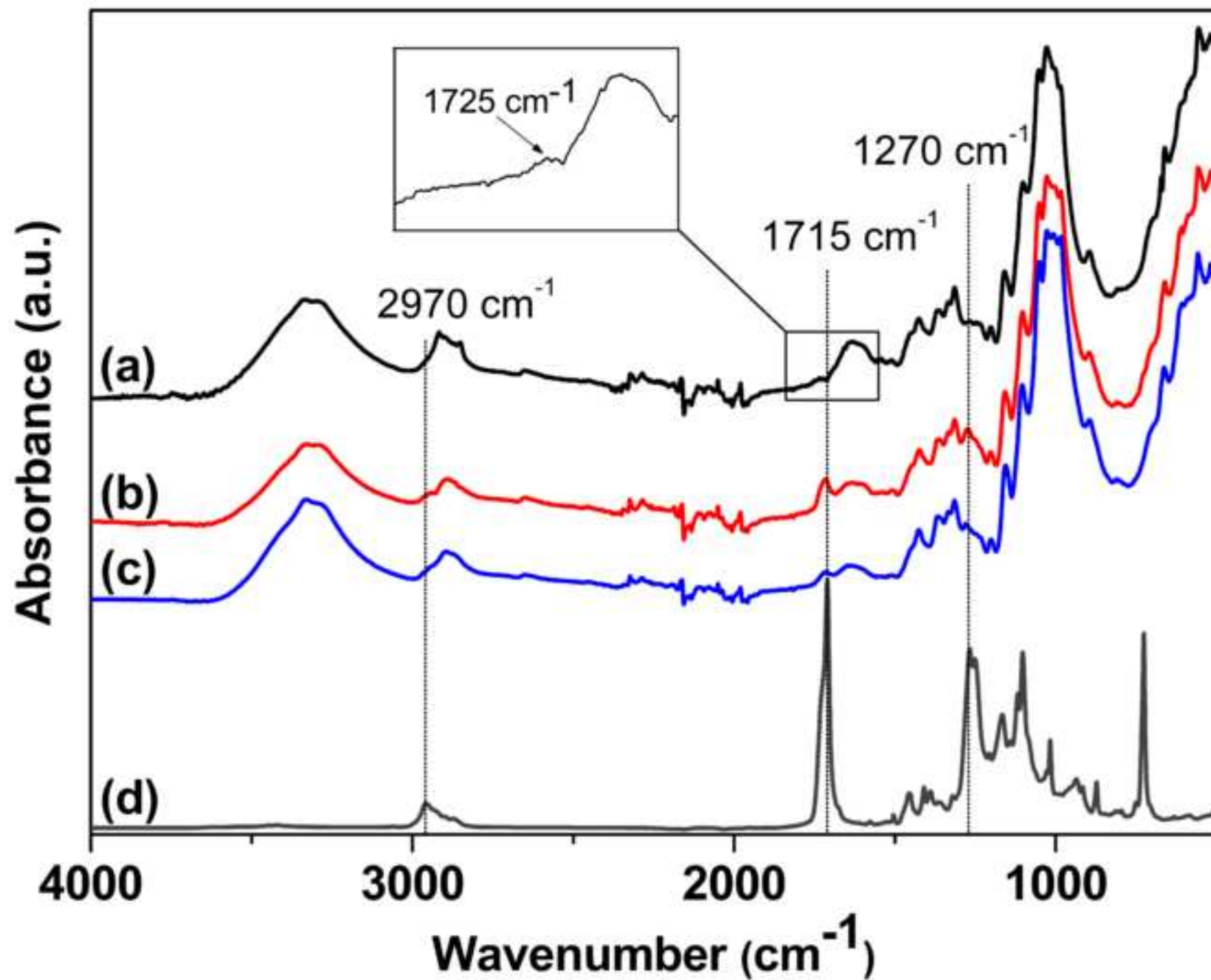


Figure 10
[Click here to download high resolution image](#)

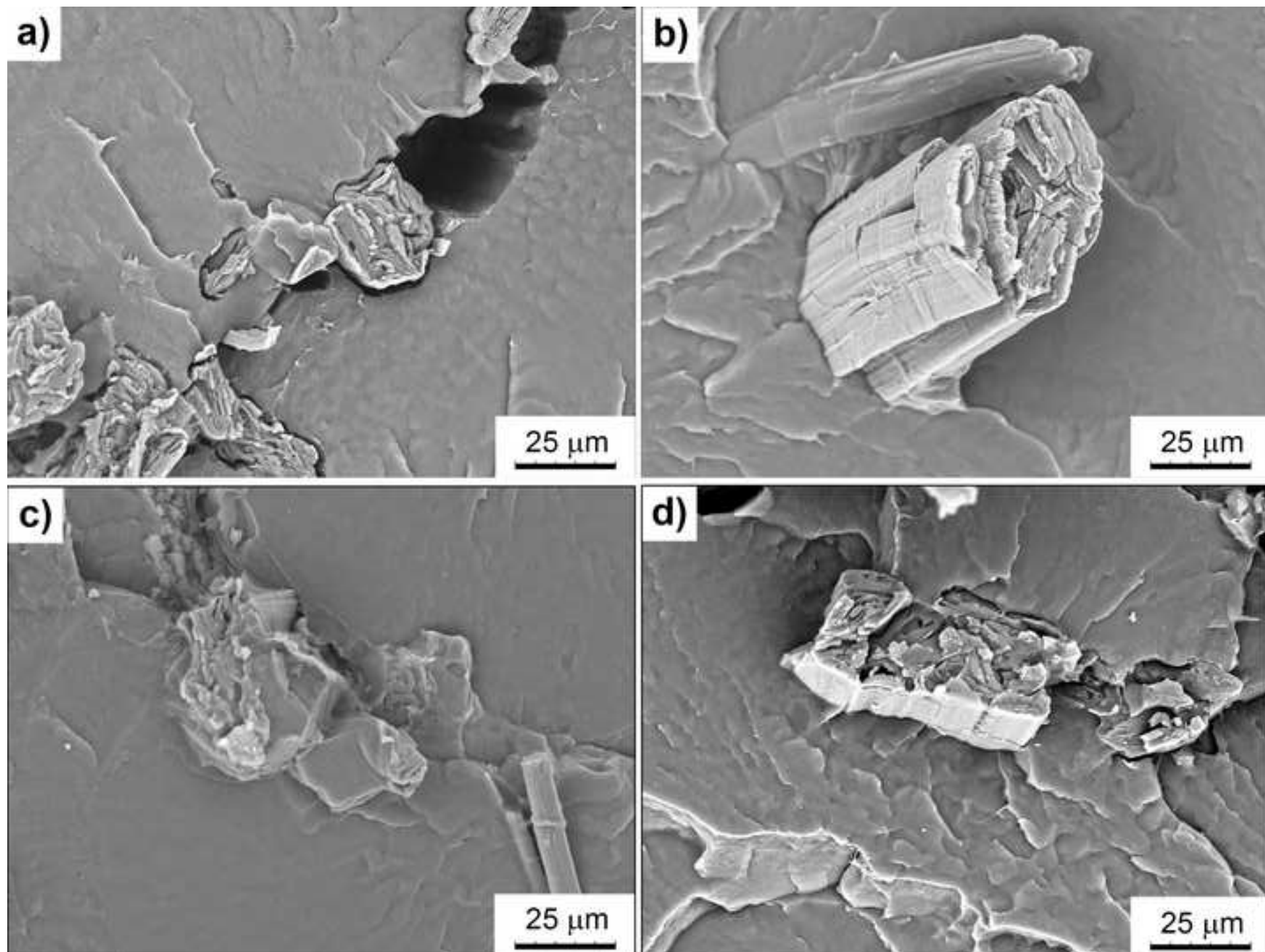


Figure 11
[Click here to download high resolution image](#)

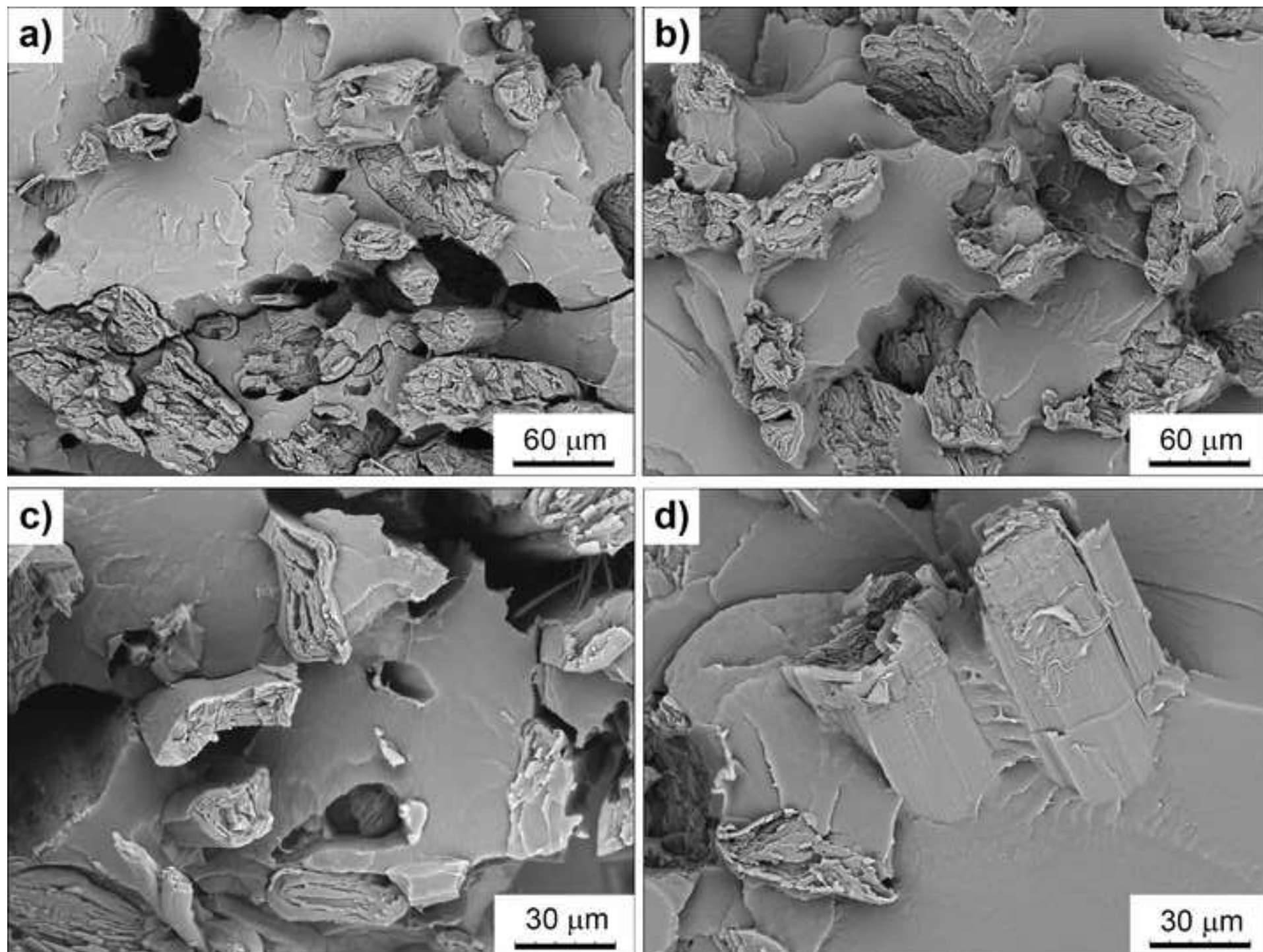
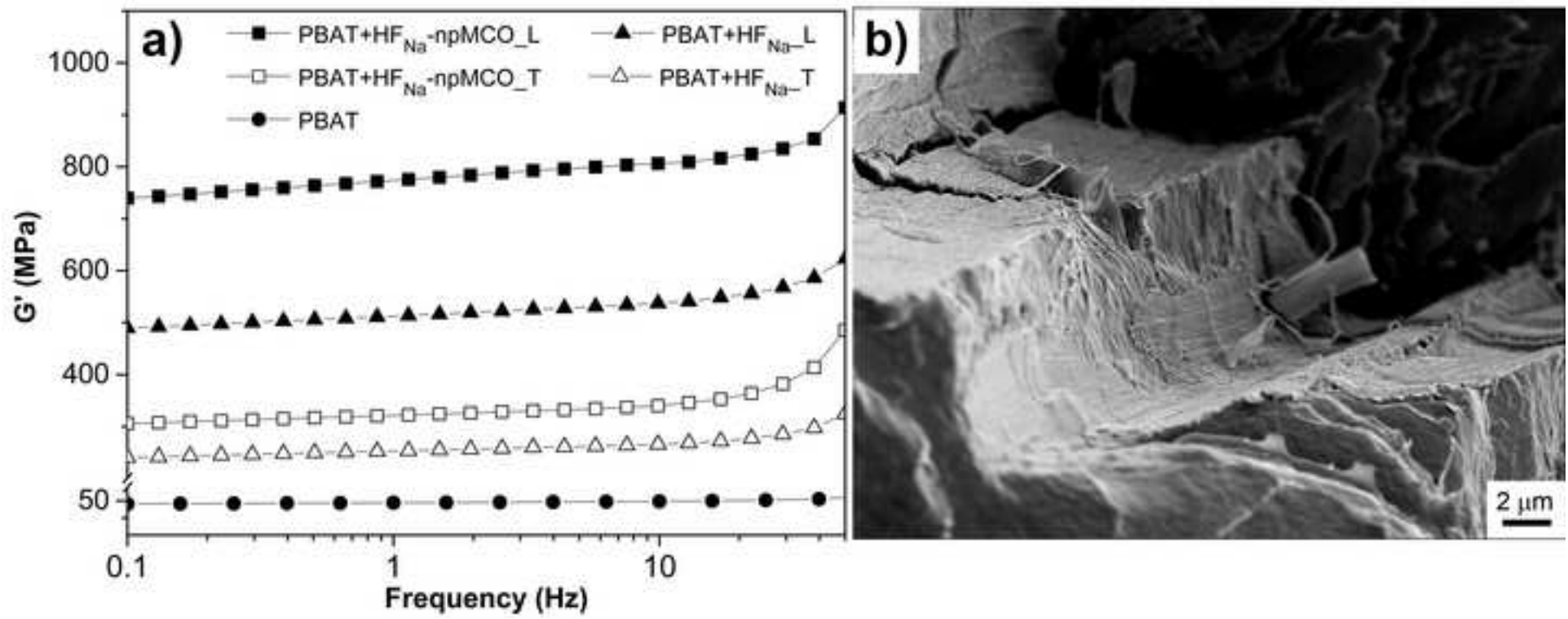


Figure 12
[Click here to download high resolution image](#)



Highlights

- Macrocyclic oligomers (MCOs) easily obtained by cyclo-depolymerization of PBAT polyester
- The MCOs easily underwent entropically driven ring opening polymerization (ED-ROP)
- Low cost hemp fibres efficiently modified with the MCOs via ED-ROP
- Good fibre/matrix adhesion in PBAT composites containing MCO-modified hemp fibres
- Good mechanical performance of the PBAT/modified hemp fibres biodegradable eco-composites